Registration No.
23676

-Technical Report-

ENHANCEMENTS AND ANALYSIS OF CTH SOFTWARE FOR UNDERBODY BLAST

Project Final Technical Report

Richard Weed[1], Christopher Moore[1], Ravi Thyagarajan[2]

[1] *Mississippi State University, Starksville, MS*
[2] *US Army TARDEC, Warren, MI*

UNCLASSIFIED: Distribution Statement A
Approved for Public Release

01 Feb 2013

U.S. Army Tank Automotive Research, Development, and Engineering Center
Detroit Arsenal
Warren, Michigan 48397-5000

REPORT DOCUMENTATION PAGE

Form Approved
OMB No. 0704-0188

Public reporting burden for this collection of information is estimated to average 1 hour per response, including the time for reviewing instructions, searching existing data sources, gathering and maintaining the data needed, and completing and reviewing this collection of information. Send comments regarding this burden estimate or any other aspect of this collection of information, including suggestions for reducing this burden to Department of Defense, Washington Headquarters Services, Directorate for Information Operations and Reports (0704-0188), 1215 Jefferson Davis Highway, Suite 1204, Arlington, VA 22202-4302. Respondents should be aware that notwithstanding any other provision of law, no person shall be subject to any penalty for failing to comply with a collection of information if it does not display a currently valid OMB control number. **PLEASE DO NOT RETURN YOUR FORM TO THE ABOVE ADDRESS.**

1. REPORT DATE *(DD-MM-YYYY)*	2. REPORT TYPE	3. DATES COVERED *(From - To)*
01 Feb 2013	FINAL	01 OCT 2010 – 31 DEC 2012

4. TITLE AND SUBTITLE

Enhancements and Analysis of CTH Software for Underbody Blast

5a. CONTRACT NUMBER
W56HZV-08-C-0236

5b. GRANT NUMBER

5c. PROGRAM ELEMENT NUMBER

6. AUTHOR(S)

Richard Weed, Christopher Moore, Ravi Thyagarajan

5d. PROJECT NUMBER

5e. TASK NUMBER
WD0037

5f. WORK UNIT NUMBER

7. PERFORMING ORGANIZATION NAME(S) AND ADDRESS(ES)

Center for Advanced Vehicular Systems, Miss State Univ
200 Research Blvd
Starksville, MS 39759

TARDEC/Analytics
6501 E 11 Mile Road
Warren MI 48397

8. PERFORMING ORGANIZATION REPORT NUMBER

9. SPONSORING / MONITORING AGENCY NAME(S) AND ADDRESS(ES)
TARDEC/Analytics
6501 E 11 Mile Road
Warren MI 48397

10. SPONSOR/MONITOR'S ACRONYM(S)

11. SPONSOR/MONITOR'S REPORT NUMBER(S)
#23676 DOC (TARDEC)

12. DISTRIBUTION / AVAILABILITY STATEMENT
UNCLASSIFIED: Distribution Statement A. Approved for Public Release

13. SUPPLEMENTARY NOTES

14. ABSTRACT

Accurate tools and procedures for simulating the blast effects of shallow buried explosive devices are critical to the Department of Defense's efforts to design blast-resistant vehicles that can increase crew survivability and counter the threat from improvised explosive devices. Of the various computer codes available for modeling explosive effects, the CTH (CHART Squared to the Three-Halves) Eulerian hydrocode from Sandia National Laboratories is one of the most popular and is considered a standard tool for blast simulations. TARDEC is using CTH as one of its tools for designing blast-resistant vehicles. Two potential areas of improvement to CTH that will enhance its value are implementation of Hybrid Elastic-Plastic (HEP) Geo-material model to support buried mine simulation and procedures for utilizing CTH-generated blast loads in LS-DYNA structural dynamics simulations. Both of these enhancements have been implemented into CTHv9.1 and tested in this project.

15. SUBJECT TERMS
CTH, HEP, DRDC, TARDEC, MSU, hydrocode, coupler, IMD, LS-DYNA, Kerley, SimBRS, ALE

16. SECURITY CLASSIFICATION OF:			17. LIMITATION OF ABSTRACT	18. NUMBER OF PAGES	19a. NAME OF RESPONSIBLE PERSON
a. REPORT	b. ABSTRACT	c. THIS PAGE			Ravi Thyagarajan
Unlimited	Unlimited	Unlimited	None	80	19b. TELEPHONE NUMBER *(include area code)* 586-282-6471

Standard Form 298 (Rev. 8-98)
Prescribed by ANSI Std. Z39.18

TANK-AUTOMOTIVE RESEARCH
DEVELOPMENT ENGINEERING CENTER
Warren, MI 48397-5000

Analytics Dept., Systems Integration and Engineering (SIE)

Feb 01, 2013

Enhancements and Analysis of CTH Software for Underbody Blast

Project Final Technical Report

By

Richard Weed[1], Christopher Moore[1], Ravi Thyagarajan[2]

[1] *Mississippi State University, Starksville, MS*
[2] *US Army TARDEC, Warren, MI*

Contents

List of Figures

List of Tables

List of Symbols, Abbreviations, Acronyms

ALE	Arbitrary Lagrangian Eulerian
APG	Aberdeen Proving Grounds, Maryland
ARL	Army Research Labs
ATD	Anthropomorphic Test Device
ATEC	Army Test and Evaluation Center
CASSI	Concepts, Analytics, System Simulation and Integration
CAVS	Center for Advanced Vehicular Studies
CotS/COTS	Commercial-Off-the-Shelf
CTH	CHART Squared to the Three-Halves
DoB/DOB	Depth of Burial
DoD/DOD	Department of Defense
DRDC	Defense R&D Canada – Valcartier
ECI	Export Control Information
EoS/EOS	Equation of State
EPIC	Elastic-Plastic Impact Computations (software) from SWRI
ERDC	Engineering Research Development Center, Vicksburg, MS
FEA/FEM	Finite Element Analysis/Method
FSI	Fluid Structure Interaction
GHULL	Generic Hull (as in TARDEC Generic Hull)
HEP	Hybrid-Elastic-Plastic
HME	Home Made Explosives
IED	Improvised Explosive Device
ITAR	International Traffic in Arms
JWL	Jones-Wilkins-Lee (as in Equation of state for explosives)
LS-DYNA	COTS structural dynamics software from Lawrence Livermore Software Corporation, CA
LS-PREPOST	COTS post-processing software from Lawrence Livermore Software Corporation, CA
M&S	Modeling & Simulation
MIG	Modeling Interface Guidelines
MPI	Message Passing Interface
MSU	Mississippi State University
POC	Point of Contact
PM	Program Manager
PRDEF	Prescribed Deformation
PRONTO	Structural dynamics software code from SNL
R&D	Research & Development
RDECOM	Research, Development and Engineering Command
RHA	Rolled Homogeneous Armor (steel)
RO	Reduced Order (as in simulations)
SimBRS	Simulation-Based Reliability and Safety
SIERRA	Suite of software from SNL
SLAD	Survivability and Lethality Analysis Directorate
SNL	Sandia National Labs, Alburquerque, NM
SPH	Smooth Particle Hydrodynamics
STL	Stereo Lithography
SwRI	Southwest Research Institute, San Antonio, TX
TARDEC	Tank Automotive Research, Development and Engineering Center
T&E	Test & Evaluation
UAB	University of Alabama at Birmingham
UBM	Underbody Blast Modeling/Methodology
WD	Work Directive
ZAPOTEC	Software code from SNL that links CTH to PRONTO3D

Executive Summary

Accurate tools and procedures for simulating the blast effects of shallow buried explosive devices are critical to the Department of Defense's efforts to design blast-resistant vehicles that can increase crew survivability and counter the threat from improvised explosive devices. Of the various computer codes available for modeling explosive effects, the CTH (CHART Squared to the Three-Halves) Eulerian hydrocode from Sandia National Laboratories, NM, is one of the most popular and is considered a standard tool for blast simulations. Several DoD agencies, including US Army TARDEC is using CTH as one of its tools for designing blast-resistant vehicles. This project incorporated two areas of improvement to CTH that will enhance its value as an analysis tool: (a) implementation of the Hybrid Elastic-Plastic (HEP) Geo-material soil model to support buried mine simulation, and (b) procedures for utilizing CTH-generated blast loads in LS-DYNA structural dynamics simulations.

Program Overview

The code enhancement and testing phases of this project were executed by Center for Advanced Vehicular Systems (CAVS), Mississippi State University, Starksville, MS (Primary Investigator: Dr. Richard Weed). The R&D effort was supported by Contract W56HZV-08-C-0236 and funded as work directive WD0037 under the Simulation-Based Reliability and Safety (SimBRS) program. TARDEC provided the requirements, test examples and overall technical monitoring and guidance to the code developers over the course of the project (Technical POC: Dr. Ravi Thyagarajan)

The program started in October 2010 and was completed in September 2012. This R&D project was funded with DoD Ancillary funding; with some partial funding for internal TARDEC resources provided by the Underbody Modeling for Testing and Evaluation project (Program Manager: Mr. Pat Horton, ARL/SLAD, Aberdeen, MD).

Summary of Accomplishments/Results

Both of the targeted enhancements to CTH Version 9.1 described in the Executive Summary have been implemented and tested in this project.

Recommendations

Both the HEP geo-material soil model and the one-way coupler to LS-DYNA have significant promise in the field of Underbody Blast modeling for IEDs. Evaluations should be continued to assess and improve these features, as well as incorporate them into future versions of CTH, including the production version released by Sandia National Labs.

These enhancements to CTH v9.1 are available to any DoD agency or industry partner with the following restriction. The CTH software is owned and maintained by Sandia National Labs, NM and has been designated Export Control Information (ECI) under the International Traffic in Arms Regulations (ITAR).

Section 1: Introduction

Accurate tools and procedures for simulating the blast effects of shallow buried explosive devices are critical to the Department of Defense's efforts to design blast-resistant vehicles that can increase crew survivability and counter the threat from improvised explosive devices. Of the various computer codes available for modeling explosive effects, the CTH (CHART Squared to the Three-Halves) Eulerian hydrocode from Sandia National Laboratories is one of the most popular and is considered a standard tool for blast simulations. TARDEC is using CTH as one of its tools for designing blast-resistant vehicles but has acknowledged a need for general user analysis support and possible enhancements to CTH that will improve its usability for TARDEC researchers. Two potential areas of improvement to CTH that will enhance its value as an analysis tool for TARDEC are implementation of material models for soils to support buried mine simulation and procedures for utilizing CTH generated blast loads in LS-DYNA structural dynamics simulations.

Although a wide array of material models are implemented in CTH, it does not support the Army Engineer Research and Development Center (ERDC) Hybrid Elastic-Plastic (HEP) Geo-material model that has proven to provide accurate simulations of the response of a variety of geo-materials to extreme loading due to blast, hypervelocity penetration, and ground shock. Accurate material models for soils and other geo-materials are critical for analysis of shallow buried explosives such as mines and improvised explosive devices. Since LS-DYNA is the standard structural dynamics analysis tool at TARDEC, implementing a procedure for transferring blast pressure loads generated by CTH simulations to LS-DYNA provides an alternative to the existing LS-DYNA Arbitrary Lagrangian-Eulerian (ALE) Fluid Structure Interaction (FSI) capability. In response to the need to improve user support for CTH and to extend the current capabilities of the code to support TARDEC buried explosive simulations, The Mississippi State University (MSU) Center for Advanced Vehicular Systems (CAVS) was awarded Work Directive WD0037 under the TARDEC Simulation Based Reliability and Safety (SimBRS) program.

This report describes research and development activities supported by Contract W56HZV-08-C-0236 and funded as SimBRS work directive WD0037 to provide CTH analysis support and code enhancements. Subsequent sections of the report will describe the objectives of the research, the implementation, verification, and validation of the ERDC HEP Geo-material model in CTH version 9.1, and the development and implementation of a coupling procedure that allows CTH pressures to be used in LS-DYNA simulations

1.1 Purpose of Project

TARDEC identified the overall objective of this Work Directive as supporting TARDEC's efforts to utilize the CTH hydrocode for analysis of blast events on Army vehicles and to design efficient systems to protect vehicle occupants by: a) providing CTH user support, b) providing CTH training as needed and c) enhancing CTH usefulness by incorporating TARDEC-identified code modifications.

1.2 Scope of the Project per WD0037

In the Statement of Work for this Work Directive, TARDEC identified two main tasks. A brief summary of the tasks and how MSU responded to them follows:

Task 1: Provide analysis support for TARDEC CTH simulations

For Task 1, TARDEC requested support for CTH analysis setup, debugging run errors, data-post processing and interpretation of results from computer simulations. MSU is committed to providing continuing support for the enhanced version of CTH developed under this Work Directive beyond the contract completion date.

Task 2: Implement enhancements to CTH to support blast simulations

For Task 2, TARDEC requested modifications to CTH to enhance the material modeling capabilities and other enhancements with emphasis on improving CTH analysis capabilities for modeling blast events on Army vehicles. Discussions with TARDEC led MSU to concentrate on two code enhancements that TARDEC deemed to be desirable and of high priority. The first code enhancement requested by TARDEC was enhancing the material modeling capabilities of CTH by incorporating the ERDC HEP Geo-Material model in CTH to improve the soil modeling capabilities of CTH for buried explosive simulations. The second code enhancement requested by TARDEC was implementation of a one-way "coupling" procedure that would allow blast pressures generated by CTH to be used in an LS-DYNA structural dynamics simulation. The bulk of the effort on this Work Directive was devoted to these two code enhancements.

The remainder of this report focuses on the progress on the two code enhancement tasks described above.

Section 2: Implementation and verification of the ERDC Hybrid Elastic-Plastic (HEP) geo-material model in CTH 9.1

2.1 Overview of the HEP model

The HEP model was originally developed by Zimmerman et al. [2] for modeling ground shock. The model was extended over the years and applied to a variety of blast and penetration problems [4, 5, 6] ERDC has fit the model to a wide variety of geological materials ranging from soils to conventional strength concretes and rocks. The model has many variants of differing level of complexity with the most commonly used variants being the simple (SHEP) and complex (CHEP) models. These models have been validated against explosive field tests for a variety of materials. ERDC maintains a library of materials fit to different model variants. These material fits were generated from quasi-static laboratory tests. The majority of the materials in the library have been fit to the SHEP model. To date, the model has been implemented in Lagrangian finite element codes such as SABER, EPIC, and PRONTO3D. To the best of our knowledge, the work described in this paper is the first successful implementation of the model in an Eulerian hydrocode.

The HEP Equation of State (EOS) model is based on a modified Tillotson equation of state [7] that calculates an energy dependent pressure-volume response for a given material. The EOS is composed of two parts, an energy independent total hydrostatic response of constituent solids, air and water and an energy dependent term. The hydrostatic part of the HEP EOS consists of multiple regions. Hysteretic unloading and reloading is modeled up to the state of total void closure or “crush”. Additional high-pressure regions and reversible solid-solid phase changes can be modeled above void closure. Non-hysteretic unloading and reloading is used above void closure. The energy independent (hydrostatic) part of the EOS depends only on the compression or volumetric strain of the material and allows for a wide variety of loading, unloading, and reloading conditions in both compression (taken as positive pressure) and tension (negative pressure). The energy dependent term allows for liquid phase transition. For shear strength, the SHEP model uses an exponential failure surface that is a function of pressure and is defined in terms of principal stress differences and constant Poisson ratios for loading and unloading which can be different values depending on the material. The CHEP model uses variable Poisson ratios but a similar yield surface. For shear modulus, the SHEP model is defined by the current compression and local bulk modulus. The CHEP module uses a spline fit for shear modulus. Figures 2.1a and 2.1b taken from Reference 5 show a representative pressure-compressibility response and yield surface for the simple HEP model. Figure 2.1a shows the various regions that can be modeled in the hydrostatic portion of the total equation of state. A more detailed description of the model can be found in Reference 3.

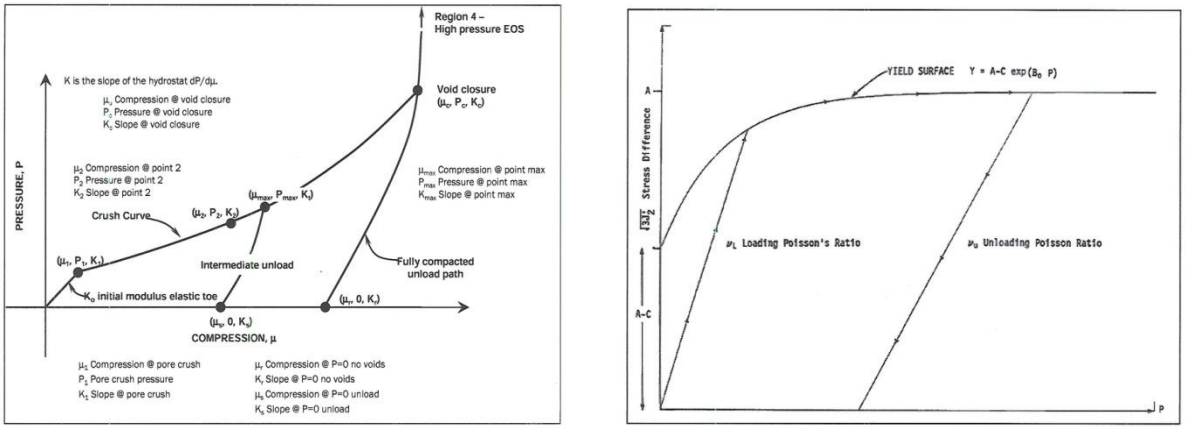

a) Hydrostatic Response b) Yield Surface

Figure 2. 1 Typical SHEP hydrostatic response and yield surface (Reference 5)

2.2 CTH HEP model implementation overview

The current implementation of the HEP model in CTH 9.1 was performed in three phases. In the first phase, software was written to implement the Simple HEP EOS and strength models as stand-alone routines. These routines were subjected to rigid unit testing outside of CTH. In the second phase of the implementation, the driver routines and supporting software required by CTH were implemented and tests were run using the CTH Prescribed Deformation (PRDEF) facility that is designed for testing new material models in CTH. The PRDEF tests were performed for three HEP soils and compared with results using an existing CTH soil modeling procedure developed by Kerley [12, 13, 14] for similar soils. In the final phase, the CTH implementation was subjected to a series of tests that compared results from CTH simulations with standard experimental results and simulation results using other models in CTH and results from the EPIC code. The following sections give an overview of the implementation of the HEP model in CTH and describe results from the PRDEF tests along with comparisons with experimental data and results from EPIC code simulations for three distinct test cases.

2.2.1 Implementation of the EOS routines

The equation of state (EOS) portion of ERDC HEP soil model was implemented using the Sandia Model Interface Guidelines (MIG) [8,9,10]. In addition, the existing Holmquist-Johnson-Cook concrete and Johnson-Holmquist ceramics models [26] were used as examples. The CTH implementation began by writing new software based on the existing literature [2,3] plus notes provided by Dr. Stephen Akers (ERDC-GSL) [11]. In addition, the implementation of the ERDC HEP model in PRONTO3D was used as a reference in the development of the new routines to resolve problems found during testing. However, none of the original ERDC software is used in the CTH HEP implementation. Based on conversations with Dr. Akers, it was decided to restrict the CTH HEP implementation to the simple or SHEP variant of the HEP model since the vast majority of the materials currently fit to the HEP model by ERDC are for the SHEP variant. The new software was written to conform to modern Fortran 2003 coding standards

and to be portable to a wide range of standard conforming compilers. Care was taken in the development of the core components of the model to insure that they can be used with minor modifications in other codes besides CTH.

The CTH EOS implementation procedure outlined in Hertel and Kerley [9] defined the CTH EOS software requirements and the existing CTH routines that must be modified to implement them. CTH requires that two forms of an EOS must be supplied to the code. Both forms are required to return pressure, sound speed, and the derivatives of pressure with respect to density and temperature and energy with respect to temperature. The two forms differ in that the first form takes in density and temperature and returns a specific energy along with the other required values while the second form takes in density and specific energy and returns a temperature. This requirement introduced three obstacles to the CTH HEP EOS implementation. The first obstacle is that the ERDC HEP EOS is cast in a form that is dependent on internal energy. Therefore, a procedure to extract a temperature that is consistent with CTH is required. The most obvious way is to assume (probably erroneously) a change in internal energy is a linear function of a change in temperature and the two are related by a specific heat at constant volume. This is the approach taken by both the Holmquist-Johnson-Cook (HJC) concrete and Johnson-Holmquist ceramic models in CTH and, until a more appropriate relationship is found, is the one used for this initial implementation of CTH HEP. However, this choice leads to the second obstacle, specifically; how to define representative values for the specific heat of soil. This information is not included in the ERDC HEP material library. The approach used to define an appropriate specific heat is given in the following section. The third obstacle was the difference in the reference conditions for thermodynamic variables used by HEP and CTH. The HEP EOS model is referenced to gage pressure but CTH uses an absolute pressure. Since the HEP model contains an energy dependent term, an “energy shift” has to be applied to the absolute energy value computed by CTH to insure that CTH will return consistent values of initial pressure and temperature. The energy shift is computed using the specific heat and a value for room temperature (298 degrees K). A similar procedure for defining a shifted reference energy state is used in the existing CTH Johnson-Holmquist ceramic model to overcome problems associated with very low or even negative energies.

Once the temperature – energy relationship was settled on and a procedure implemented for defining a specific heat, two driver routines were written that take in the required dependent variables and then call the base HEPEOS routine to return pressure and the other required values. Since the HEP models use Mbar as the unit of pressure, the pressure and energy terms are scaled on entry to and exit from the driver routines to take in and return the default CTH force units of dynes. The next step was to define the required extra or history variables that must be carried over from the previous time step. The SHEP EOS implementation only requires one history variable, the maximum value of the compression or volumetric strain for each cell. The strength model requires at least one more extra variable, the derivative of pressure with respect to compression. For the initial implementation we are only defining the maximum compression over time. Next a material number based on the range of available material numbers in CTH was selected. For the current CTH HEP implementation, the both the Equation of State and Elastic-Plastic model material numbers was set to 27. The last tasks before final implementation of the model were to create a data check routine to initialize computed constants and check input data,

write an extra variable routine that is used to register the extra variable with the CTH database and modify a relatively small group of CTH routines to include the new model. The only other modifications were the addition of a module routine that holds the global variables for the HEP model along with some support routines and updating the existing CTH make files to include the new software in the compilation. A more detailed description of the new subroutines that make up the HEP EOS model and the changes made to existing CTH routines is given in Appendix A.

2.2.2 Strength model implementation

The constitutive model was implemented in CTH as a "traditional" total stress model that is based on Von Mises J2 plasticity. The HEP routines supply CTH with a value of the material yield surface based on the deviatoric principle stresses and an estimate of shear modulus. CTH weights these values with the volume fraction of the material and sums these values with the values for other materials in a cell that can support material strength to produce a cell value for shear modulus and yield strength. Following the Johnson-Holmquist ceramic model implementation, a set of seven include files were developed that define the number of variables used in the model, the extra variables required by the model, and a driver routine that calls the HEP yield surface and shear module routines. As with the EOS component of the HEP model, a more detailed description of the code and changes to existing CTH software is given in Appendix A. Although soils in general have little strength in tension, the constitutive model plays an important part in the values of impulse and crater geometry generated by the HEP model for soils with low adhesion such as dry sand.

2.2.3 The GenCTHInput utility

In addition to the CTH software, an utility (named GenCTHInput) was written to translate HEP model inputs provided by ERDC in an input file format used in EPIC and PRONTO3D into a format that can be read by the standard CTH input routines. GenCTHInput is a standalone code written in Fortran 2003 and will be provided with the enhanced version of CTH 9.1. This utility was written to allow for the addition of new HEP materials not included in the current ERDC HEP library. In addition to translating the EPIC and PRONTO3D format files into a format the CTH can read, GenCTHInput computes the value of material specific heat using the procedure described in the next section. The GenCTHInput utility will be described in more detail in the Users Manual that will accompany release of the enhanced version of CTH.

2.2.4 Definition of soil specific heat values

A survey of existing literature on the thermal properties of soils revealed that the most common procedure for estimating the volumetric heat capacities or specific heats of soils was introduced by De Vries [16]. De Vries computes the volumetric heat capacity of a soil as a sum of the heat capacities of the individual soil constituents, the heat capacity of water scaled by the gravimetric water content, the heat capacity of air based on the void fraction of air in the soil, and the heat capacity of the organic matter in the soil. Several researchers [17,18,19] use a reduced form of this approximation that involves a mean value for the dry soil constituents (usually taken to be in the range of 0.73 kJ/kg/K to 0.837 kJ/kg/K), the

heat capacity of water (4.180 kJ/km/K), the dry bulk density of the solids and the soil water content in terms of weight fraction. The form of the equation for the heat capacity then becomes:

$$\rho c_v = \rho_b (c_s + c_w w) \qquad \text{(Eq. 1)}$$

where ρc_v is the volumetric heat capacity of the soil, ρ_b is the dry bulk density for the soil, c_s is the specific heat of the dry soil solids (taken to be 0.837 kJ/kg/K for this report), c_w is the specific heat of water (4.184 kJ/kg/K where the density of water is 1 gm/cc) and w is some approximation of the gravimetric moisture content of the soil (kg/kg). This can be either the water content in percent measured by experiment or the ratio of the dry to wet material densities. The option to use this equation or input a specific heat value directly is included in the GenHEPInput utility which will convert the results into the CTH units for specific heat of ergs/g/ev where ev is an electron volt which is equivalent to 11604.5 degrees Kelvin. For the soils shown in Table 2.1, this procedure leads to values of Cv on the order of 1.1E11 to 1.7E11 ergs/g/ev. These values are consistent with Cv values of other materials in the CTH material database. An important point to note is that the specific heat value computed by this procedure is primarily a function of the moisture content of the soil. Typical values for the wet and dry densities along with water content and percent air voids are given in Table 2.1 for the six HEP materials used in this report.

Material Description	ERDC Material Classification	Soil Classification	Air Voids, %	Wet Density, Mg/M^3	Dry Density, Mg/M^3	Water Content, %
Gravelly Clay	WCLAY1	CL	3.9	1.96	1.59	23.7
Clayey Sand	ISOIL1	SC	12.0	2.02	1.80	12.1
Concrete Sand	DSOIL1	SP	26.5	1.86	1.79	4.0
Clay	IMD WET CLAY	CL	3.4	1.97	1.59	24.0
Silty Sand	IMD INT SOIL	SC	10.9	2.01	1.84	12.7
Dry Sand	IMD DRY SAND	SP	29.8	1.77	1.70	3.8

Table 2.1. Properties of Six ERDC HEP soils

2.3 Verification testing of the HEP model implementation

2.3.1 Unit testing of the CTH HEP model software

A unit test driver for the new HEP software was written to exercise the software outside of CTH. This testing was a critical part of the development process because it helped identify bugs that would have been hard to diagnose in a standard CTH run. The driver allowed the EOS, yield surface and shear modulus components to be tested using either a user defined strain history or input from a CTH run. The user defined strain option allowed for the definition of multiple unloading-reloading paths. The objectives of the tests were to reproduce Figures 5 and 6 from Reference 4 and compare results with the output from the ERDC HEP routines. These results are shown in Figures 2.2a and 2.2b for the gravelly clay, clayey sand, and concrete sand data HEP materials. The exact correlation between the new routines and the old ERDC routines indicated that the initial implementation of the hydrostatic part of the EOS and the yield surface was correct.

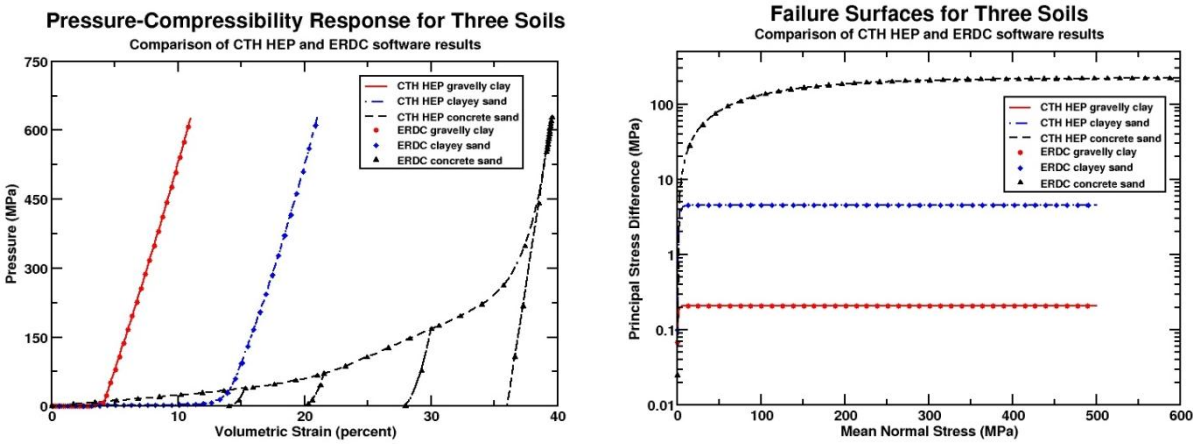

a) Hydrostatic Response b) Yield Surface

Figure 2. 2: Comparison of CTH HEP and ERDC software results for hydrostatic response and yield surface

2.3.2 CTH Prescribed Deformation (PRDEF) test: Results and Discussion

A next set of tests were run following a suggestion by Dr. Akers to use the CTH Prescribed Deformation (PRDEF) option to mimic a uniaxial compression test in CTH. The PRDEF option allows the user to run CTH with a user specified strain time history using different strain measures. PRDEF is designed for testing CTH EOS and strength models separate from the other parts of the code. The strain history used for these tests was taken from a CTH example problem and is shown in Figure 2.3. Tests were run using the HEP model fits for the WCLAY1 and DSOIL1 materials and compared with results for similar soils using inputs developed by Kerley [12. 13. 14]. The Kerley reports outline a procedure for using existing CTH SESAME EOS tables [8] for soils with various water contents generated by Kerley to

model some of the soils in the HEP database. These tests resulted in the pressure versus strain and pressure versus time results shown in Figures 2.4a-2.4d for the WCLAY1 and DSOIL1 materials. The CTH HEP implementation is seen to agree well with the Kerley model for the wetter material (WCLAY1) but to yield substantially different results for the dry sand material (DSOIL1). However, it has been demonstrated by comparisons with experimental results that the Kerley fit is not a good model for this material. These results demonstrated that the CTH HEP implementation delivered equal or better material response for an arbitrary strain history when compared to the Kerley models.

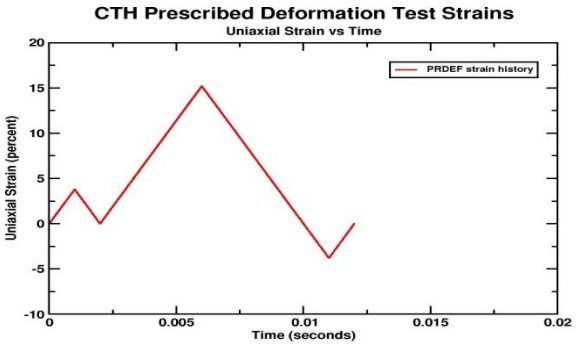

Figure 2. 3: Strain vs time history for PRDEF tests

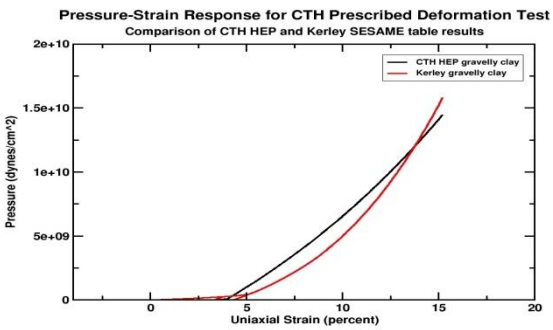

2.4a) WCLAY1 P vs Strain

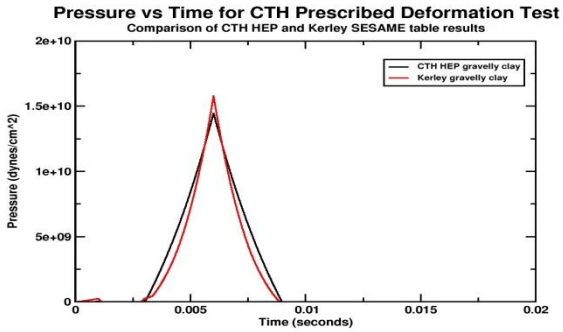

2.4b) WCLAY1 P vs Time

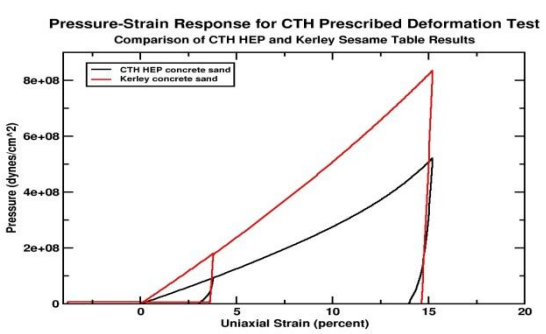

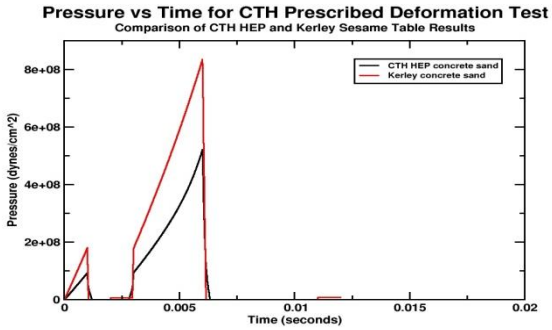

2.4c) DSOIL1 P vs Strain

2.4d) DSOIL1 P vs Time

Figure 2. 4: PRDEF Hydrostatic Response of CTH HEP and Kerley Soil Models for WCLAY1 and DSOIL1 materials

2.3.3 Pioneer buried explosive simulations

Initial pioneer testing with the CTH HEP implementation was performed using the test problem described in Kerley's reports along with a similar test case used by Littlefield [15] to compare results from the EPIC HEP implementation with CTH runs using Kerley's model. Both test cases simulate blast effects on a witness plate suspended over a shallow-buried explosive charge. Cases for three HEP soils were run with the Kerley inputs as well as the new HEP model and the results were compared. The CTH HEP results were also compared with results presented by Littlefield that compares results using the Kerley SESAME model in CTH results with the EPIC code using the HEP model for a witness plate simulation similar to the Kerley tests.

2.3.3.1 Kerley test case: Results and Discussion

The initial tests for the CTH implementation were performed using the test case described by Kerley [13] for the three soils mentioned previously. The test case consists of a 20 cm thick witness plate of RHA steel with a diameter of 276 cm suspended 46 cm above a soil mass that is 124 cm deep and 368 cm wide. A 9217 g (20.32 lb) charge of TNT is buried in the soil at a depth of burial of 16 cm. The TNT is taken to be a cylinder with a radius of 15 cm and a height of 8 cm. The TNT is modeled in these simulations using the JWL equation of state. Kerley suggests using a procedure that allows the SESAME table values for the TNT detonation products to be used in place of JWL in order to avoid potential problems with JWL at low pressures but JWL was deemed sufficient for these tests. The RHA steel plate is modeled using the SESAME EOS for RHA steel along with the CTH elastic-plastic model and the Johnson-Cook fracture model with a strength in tension of -3.8E10 dynes/cm^2. All tests were run in 2D cylindrical coordinates using a constant mesh spacing of 1 cm in both directions. Half-symmetry was assumed to reduce the size of the problem space.

The three soils were modeled using the SESAME table inputs generated by Kerley [13]. Kerley's model takes SESAME tables that were generated for soils with various water contents and then adjusts them with the CTH p-alpha porosity model to match the dry density, porosity, and water content of the three soils used in these tests. The model attempts to match as closely as possible Hugoniot data obtained

from ERDC and other sources. Since the HEP strength model was not implemented at the time of these initial tests, the elastic-plastic and CTH geo model inputs suggested by Kerley were used to model the shear response of the three soils for both the Kerley input and the CTH HEP simulations.

Simulations for all three soils were performed with simulation times that ranged from 3 ms to 5 ms. The 3ms simulations were used to compare with the material plots given by Kerley for the three cases. The 5 ms simulations were used to compare impulse time histories for RHA plate. Impulse for these correlations was taken to be equivalent to the total Y momentum of the RHA material. The three cases using the Kerley SESAME input were run first followed by the same cases using the CTH HEP model. The only change in the inputs was to replace the SESAME EOS input for each soil with its equivalent CTH HEP input. Figures 2.5a-2.5f compare the combined material and pressure plots for the Kerley model and CTH HEP at 3.0 milliseconds for each of the three soils. The material plots are the left half-plane of the figures. Comparison of the Kerley results with the results given in his report and with the CTH HEP results revealed some interesting differences. First, the Kerley results for CTH V9.1 do not match the results for the older CTH99 version used in his report. In particular, there appears to be more soil material in regions

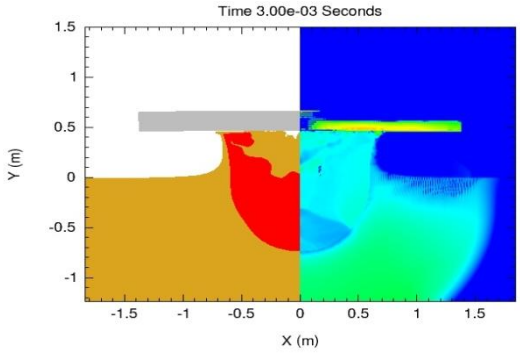

2.5a.) Kerley – Clayey Sand

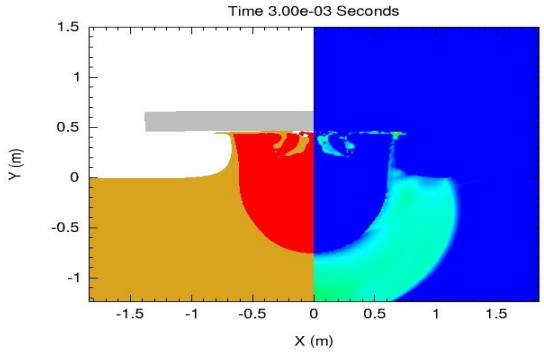

2.5b.) HEP – Clayey Sand

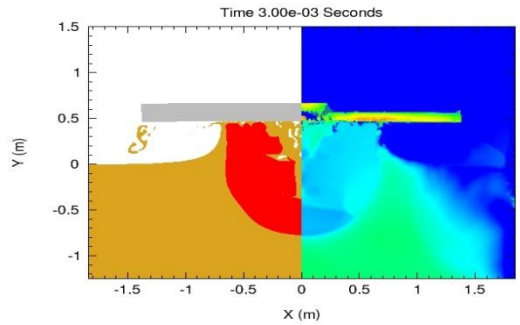

2.5c) Kerley – Gravelly Clay

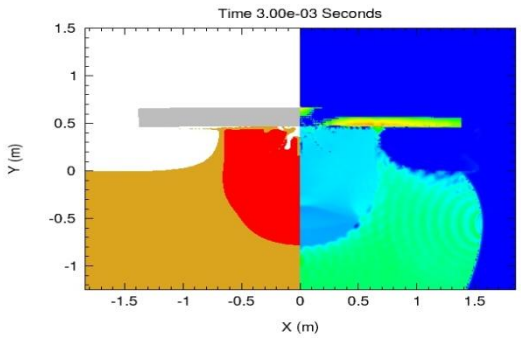

2.5d.) HEP – Gravelly Clay

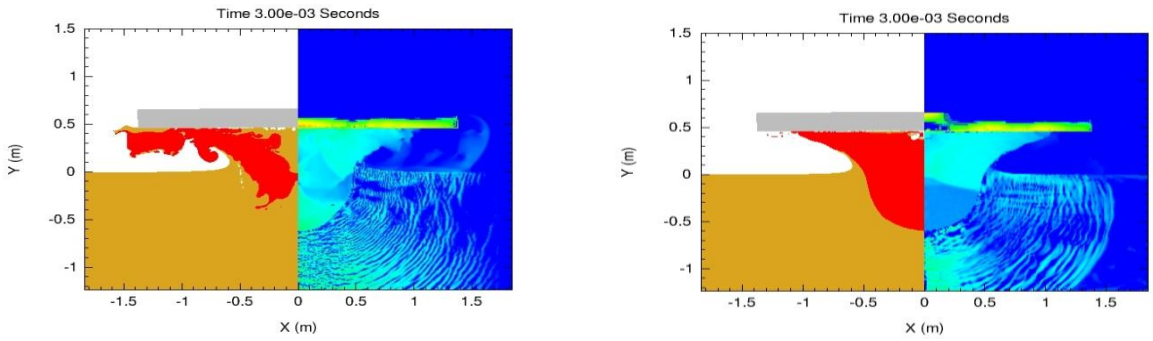

2.5e.) Kerley – Concrete Sand

2.5f.) HEP – Concrete Sand

Figure 2. 5: Comparison of Kerley and HEP crater results for Kerley test case at 3.0 ms

where the older version of CTH shows detonation products. However, the CTH HEP results appear to more closely match the CTH99 results than the results using CTH V9.1 with Kerley's inputs. Littlefield [15] saw similar differences in the simulations he ran to compare with the EPIC Lagrangian code. A set of CTH material discards that removed some soil material at very low pressures were required to yield material plots that matched the EPIC results. It is felt we are encountering a similar problem with the Kerley test case. The effect of removing the low-pressure material will be illustrated in a following section where a comparison with results generated by one of Littlefield's test cases will be presented.

As observed by Kerley, the concrete sand material which has the lowest water content of the three soils (see Table 2.1) and the highest yield strength has the lowest amount of lateral containment of the detonation products by the soil. The moister soils (designated gravelly clay and clayey sand) show considerable lateral containment of the detonation products. The effect of the increased amount of lateral containment can be seen in the comparison of impulse versus time for the three soils given in Figure 2.6. The moister soils are seen to generate much higher impulse on the witness plate. The excess amount of soil material in the CTH V9.1 results makes estimates and comparison of crater dimensions difficult. However, a visual comparison of the CTH HEP results with the CTH99 results in Kerley's report shows that CTH HEP is giving similar crater sizes. In general, the correlations for the gravelly clay and clayey sand look very good with the clayey sand case giving an excellent correlation for impulse. The concrete sand material correlations can be characterized as fair to good at best.

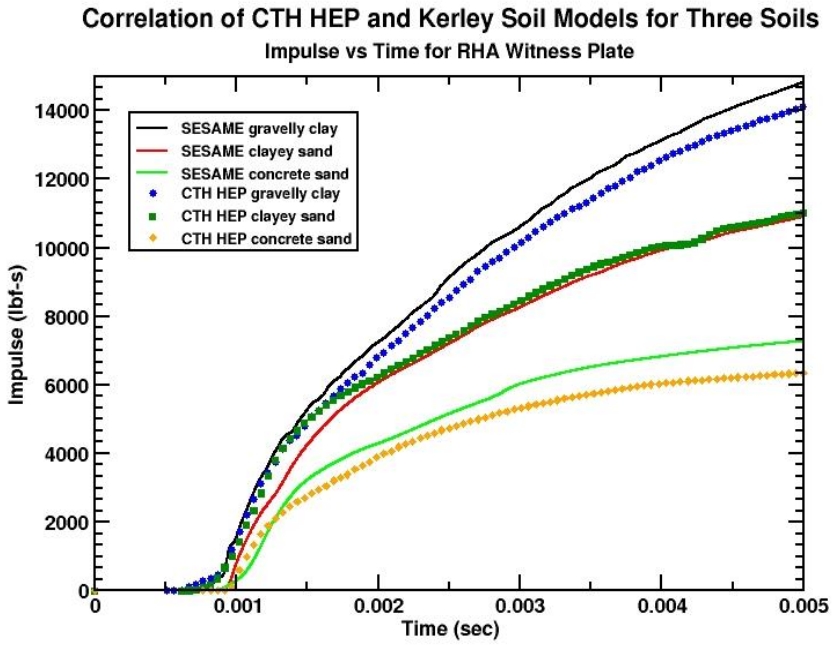

Figure 2. 6: Correlation of impulse on a witness plate using CTH HEP and Kerley soil models for three test soils

Another interesting result of these tests is that the CTH HEP EOS appeared to be more stable than Kerley's model. The clayey sand case would not run with Kerley's inputs without using material discards to remove material with negative energies and densities. All the cases run with the CTH HEP model ran to the specified stop time without discards. However, subsequent tests did require discards for stable simulations with the HEP model.

2.3.3.2 Littlefield test case: Results and Discussion

Dr. David Littlefield (UAB) compared of Kerley's model for the three soils used in this report with results from the EPIC code [15]. Dr. Littlefield provided input decks for his Kerley model comparisons along with impulse data from the EPIC code. Littlefield's test case was run using the WCLAY1 and DSOIL1 HEP inputs and compared with his results for Kerley's model and EPIC. The material discards criterions provided in Dr. Littlefield's input were used to provide a better visual estimate of the crater depth and diameter generated by the CTH HEP model and to provide data to compare with the EPIC and CTH results using Kerley's input. Dr. Littlefield's test case differs slightly from the Kerley test case, primarily in the extent of the computational domain and the depth of burial of the charge. For these tests the charge is buried 10 cm below the soil surface instead of 16 cm. Also, the Johnson-Cook model for steel was used for the strength model. A tensile fracture stress of -3.018E9 dynes/cm^2 was used for the CTH fracture model. Results were generated using the CTH HEP model with the material strength model used by Kerley and the HEP strength model. The initial material configuration for Littlefield's test case is shown in Figure 2.7. Material response and pressure at 3 ms are shown in Figures 2.8a and 2.8b for the WCLAY1 material. The computed impulse for the two models is compared with EPIC results in Figure 2.9. The results in Figure 2.9 illustrate both the minimal effect of the CTH strength model for the

WCLAY1 material and the improved accuracy of the Eulerian solution over the Lagrangian solution generated by EPIC when the material behaves more like a fluid than a solid. These results are contrasted with the results shown in Figures 2.10 and 2.11 for the dryer DSOIL1 material. The computed impulse from the CTH HEP model and the results from EPIC are in excellent agreement. The Kerley inputs for this case under-predicts the impulse. With material discards in place, the resulting material plots for both materials show good agreement for the depth and diameter of the crater.

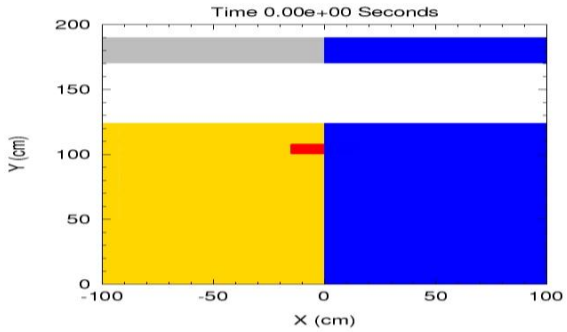

Figure 2. 7: Initial material configuration and pressure for Littlefield test case

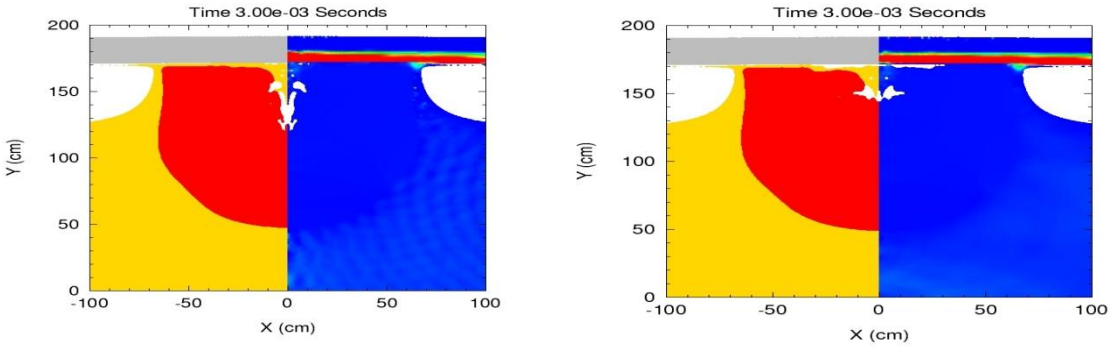

2.8a) CTH HEP

2.8b) Kerley Model

Figure 2. 8: Littlefield test WCLAY1 material response and pressure at 3ms for CTH HEP and Kerley models

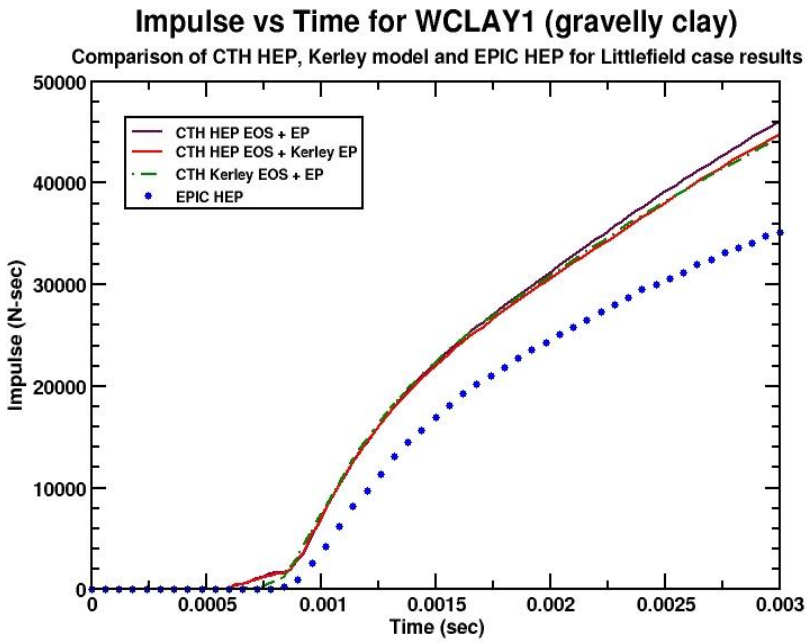

Figure 2. 9: Correlation of Littlefield test WCLAY1 impulse for CTH HEP and Kerley models with EPIC results

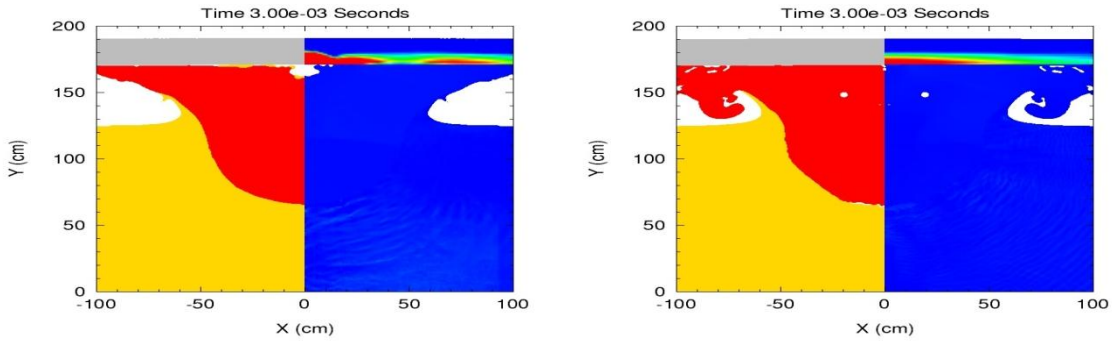

2.10a) CTH HEP 2.10b) Kerley Model

Figure 2. 10: Littlefield test DSOIL1 material response and pressure at 3ms for CTH HEP and Kerley models

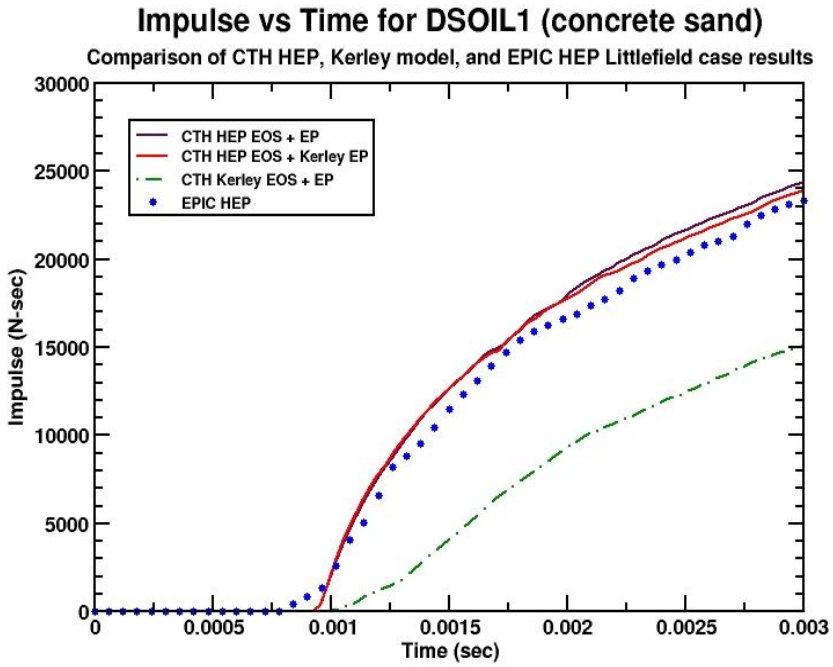

Figure 2. 11: Correlation of Littlefield test DSOIL1 impulse for CTH HEP and Kerley models with EPIC results

2.4 ERDC Impulse Measurement Device (IMD) simulations

The final sets of validation tests for the HEP model were run using the three soils tested in the ERDC Impulse Measurement Device (IMD) [20]. The majority of the results generated for these tests used a simplified version of the IMD geometry in which the mass of the piston and guide rails of the IMD device were modeled by increasing the height of the target plate component to match the overall mass of the system. The simplified geometry was adopted to limit the extent of the computational domain so that runs could be made on relatively course grids to improve turnaround times for the tests. Simulation of the explosive process was limited to the CTH programmed burn model and the JWL equation of state. In addition, only the soil in the test bed was modeled. A more detailed CTH model of the IMD experiment was obtained from Dr. Greg Bessette (ERDC/GSL) [25] late in the program that includes part of the piston assembly and models both the test bed soils and the surrounding *in situ* soils. The CTH input file provided by Dr. Bessette contained a fit of the IMD WET CLAY material obtained using the Kerley SESAME tables and P-alpha porosity corrections. The explosive detonation process is modeled using a reactive burn model instead of JWL. Due to time and budget constraints only the WET CLAY case was run using Bessette's detailed model of the IMD test configuration.

For all IMD test cases, the computed impulse and crater dimensions for the buried charge cases were compared with the experimental values and the EPIC calculations performed by Moral et al. The HEP material model data for the three soils and the EPIC impulse results were obtained from ERDC. The following sections present an overview of the IMD experiments, the three soils used in the test and results obtained from the simulations.

2.4.1 Overview of the ERDC IMD facility

The ERDC IMD facility shown in Figure 2.12 was designed and built by ERDC under TARDEC funding to obtain data on the aboveground environment created by the detonation of shallow-buried explosives. The facility was designed to obtain data on overpressure, impulse, and ground shock for different soil types. A complete description of the IMD facility, the testing procedures and instrumentation, and the test conducted with the facility is given in Reference 20. ERDC developed three test soils for the IMD experiments that were based on the WCLAY1, ISOIL1, and DSOIL1 materials [21,22,23]. The IMD experiments included above ground, partially buried (surface tangent), and shallow buried (Depth of Burial of 4 inches) detonations in three soils of different type and water content. In addition to impulse measurements, side-on pressure and ground shock data was obtained. The results presented in the following sections will concentrate on the shallow buried cases since they were deemed to be of the most immediate interest to TARDEC. The ERDC IMD experiments represent the most complete set of data on the effect of soil types and explosive Depth of Burial (DOB) to date and provide an invaluable resource for validation of soil models used in blast simulations. The distance from the bottom of the plates to the top of the charge was maintained at 20 inches for all the test configurations.

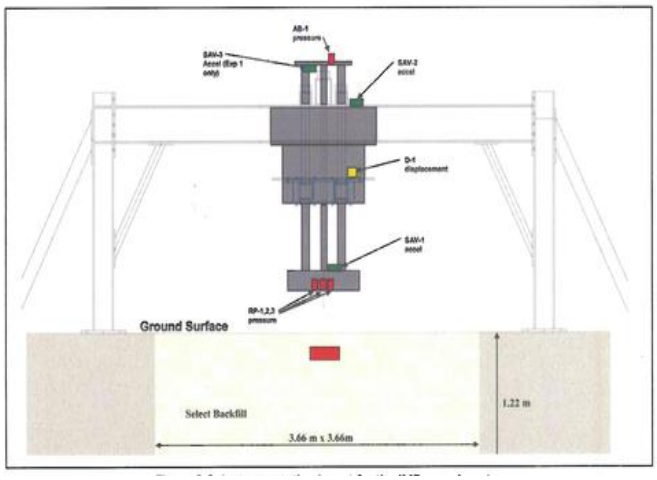

Figure 2. 12: Schematic of ERDC Impulse Measurement Device (Reference 20)

2.4.2 Description of the three IMD soils

The three soils tested in the IMD facility consisted of a wet clay material, and intermediate soil described as “silty sand”, and a dry sand material. Table 2.1 presents the material densities and water content of the three soils. ERDC characterized these three materials and fit the material properties to the Simple HEP (SHEP) model. These material fits were used by Moral et al. [5] in EPIC simulations that compared the computed impulse with the experimental values. These fits were obtained from Dr. Moral

and used in the CTH HEP simulations without modification. CTH input files for the three soils were generated using the GenHepInput tool. As shown in the results presented in the following sections, the soil type (in particular the water content) along with the DOB has a dramatic effect on the amount of impulse.

2.4.3 Simulation of the ERDC IMD experiments with a simplified geometry

A set of simulations were run using the CTH HEP model with the goal of comparing the results for impulse and crater geometry for a shallow buried explosive with Ehrgot's experimental results and Moral et al.'s EPIC simulations. Simulations were run using a 5 lbm charge of C4 at a DOB of 4 inches for the three soils tested in the IMD, as reported in Reference 20. The CTH simulations used a 2D cylindrical grid with a constant mesh spacing of 1 cm in both the radial and axial directions. Only the IMD target plate assembly was modeled due to the difficulty of modeling the guide pistons and the rest of the IMD structure in CTH. The thickness of the target plate assembly was adjusted to account for the total mass of the IMD (5500 lbm). The SESAME EOS for 4340 steel was used for the target plates. Due to the lack of specific values for 4340 steel, the Johnson-Cook default values for steel were used for the CTH constitutive model. The JWL EOS was used to model the explosive. As previously stated, the soils were modeled using the HEP model fits supplied by ERDC. The surrounding air was modeled using the SESAME tables for air. Half symmetry was used to reduce the problem size. Semi-infinite boundary conditions were used at the bottom, top, and right boundaries. A second set of runs was repeated using with the mesh spacing refined to 5 mm in both directions to quantify the effect of mesh spacing on the results. The effects of CTH inputs such as the multi-material cell pressure formulation (MMP) and cell fracture (actually spall) parameters were also investigated. The initial material configuration for all the CTH simulations is shown Figure 2.13.

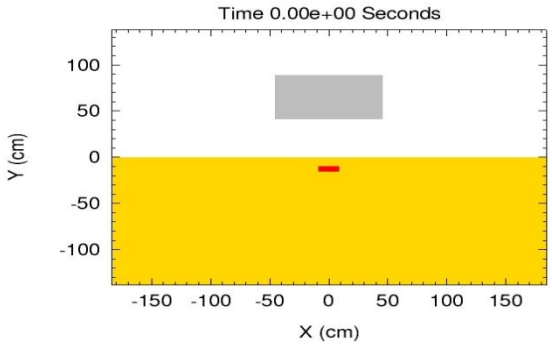

Figure 2. 13: Initial material configuration for CTH HEP IMD simulations

Initial simulations were run using the default CTH MMP option (MMP0) with the default values for material strength mixture parameter (MIX 1). The pressure form of the PFRAC input was used with the PFRAC value for the soil set to a small value of -1.E-4 dynes/cm^2. In the absence of a specific material fracture model such as the Johnson-Cook model, CTH will use the values of PFRAC to define a tensile pressure at which a material is considered to have fractured and spalled. CTH uses this pressure (or stress) to determine when void material is introduced into the cell. This induces a change in volume in each material of the cell that has a pressure more negative than a "relaxation" value that is a fraction of

the fracture criterion for the cell. CTH also allows the PFRAC values to be specified as a principle stress value that is converted to a pressure value inside the code. However, the pressure form of the PFRAC input is the preferred input format for CTH. This introduces a problem with the HEP model due to the reference of the pressures generated by the model to gage pressure. The hydrostatic (compression dependent) term in the HEP EOS allows small values of negative pressure (tension) to be generated during unloading. However, when these values are referenced to absolute pressure by adding the gage pressure (1 atm), they will longer be negative. The results obtained to date indicate that the simulations will still run and produce realistic results but the exact effect of using the pressure based PFRAC is still under investigation. Results were also generated using the stress form of PFRAC but showed only small changes in results.

2.4.4 Results for 1 cm mesh with strength

The impulse of the IMD target obtained for the three soils are compared with the experimental values obtained by Ehrgot [20] and the EPIC results of Moral et al. [5] for the default 6 mm mesh spacing given is shown in Figure 2.14. On examination of the experimental values tabulated in the Ehrgot's report, it was found that the experimental value for peak impulse used by Moral et al. for the dry sand material was higher (7740 N-s versus 7273 N-s) than the value given in Ehrgot's report. The lower experimental value for impulse of the dry sand is shown in Figure 2.14. For the dry sand material, CTH HEP under-predicts the impulse by about 15 per cent. EPIC over-predicts the impulse for the 6 mm mesh spacing. For the wet clay material, CTH HEP yields a better correlation with experiment than EPIC. Impulse for the wet clay material is slightly over-predicted by CTH HEP and under-predicted by EPIC. For the intermediate soil material, both EPIC and CTH HEP over-predict the impulse in comparison with experiment with the CTH HEP results closer to experiment. .

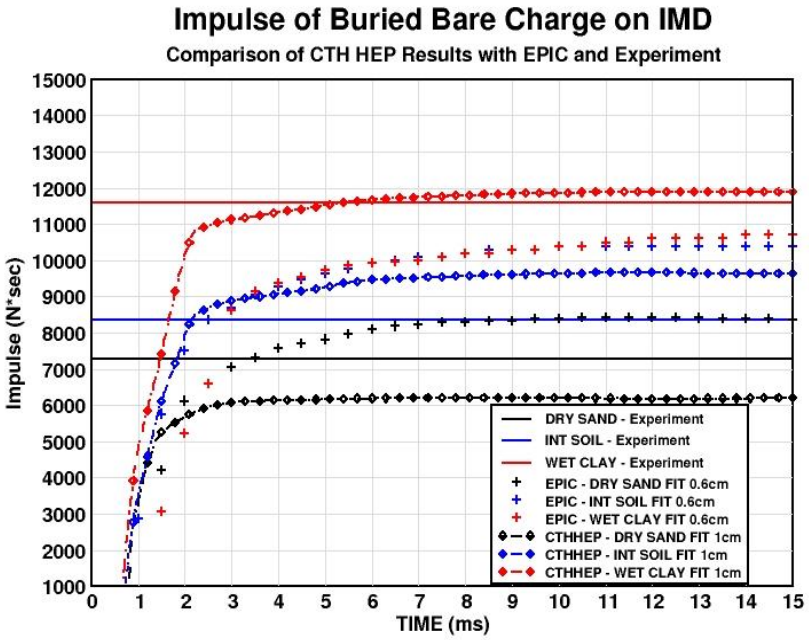

Figure 2. 14: Correlation of CTH HEP and EPIC impulse on IMD for course mesh with experiment

Figure 2.15 is taken from Reference 20 and shows the measured crater dimensions for the experiments. Material plots for the three materials at 15ms simulation time are given in Figures 2.16a-2.16c. These results demonstrate the importance of the strength and failure models used in the simulations and the effect of soil cohesion on the results. The wetter materials have much lower shear strength but higher cohesion than the dry sand. This leads to more lateral confinement of the blast for a longer period of time for the wetter materials Visual comparison of the CTH result with the experimental results shown in Figure 2.15 indicate that CTH HEP is doing a good job of predicting the crater depth and as well as the overall shape of the crater. The dry sand results are of particular interest because they are another indicator of the effect of the strength model. The relatively flat section of the crater floor is captured along with the shallow slope of the crater wall. However, the crater diameter appears to be under-predicted. Experience has shown that trying to interpolate crater geometry from CTH material plots should be done with caution because the image presented can be greatly affected by the use of material discards that are a necessary evil in many CTH calculations to insure a stable solution. A better method for computing the crater dimensions based on material volume fraction is being investigated. The material plots for the wet clay and intermediate soil materials show the steeper crater slopes and lateral containment of the blast that is expected due to their higher cohesions. Crater depths for these two materials are also close to the experimental values.

2.4.5 Results for 5 mm mesh with strength

In order to determine the effect of mesh density on results, a second set of simulations were run with the CTH mesh size decreased to 5 mm in both directions. The impulse values are compared with EPIC results using a 3 mm mesh and experiment in Figure 2.17. The effect of mesh refinement on the CTH results is to shift the impulse values down to lower peak values. This moves the wet clay results slightly below the experimental values. The intermediate soil values move closer to the experiment but still over-predict the impulse. The dry sand values show a slight downward movement. It is interesting to note that the EPIC results show a similar effect for grid refinement from 6 mm to 3 mm. EPIC continues to provide a better prediction for the dry sand case indicating that the strength and failure models in EPIC are providing a more realistic result for this soil. In contrast, the EPIC and CTH results for the intermediate soil are now very close.

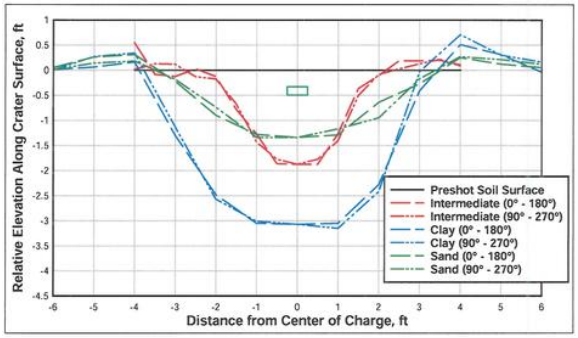

Figure 2. 15: Experimental crater dimensions (Ref. 20)

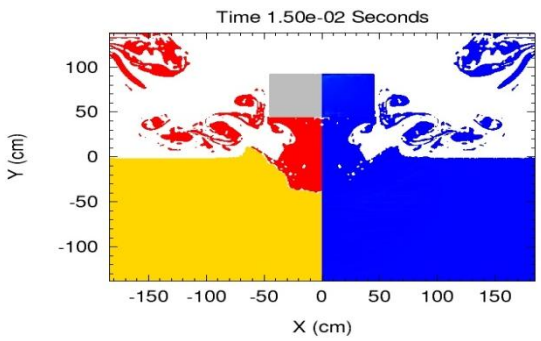

2.16a) IMD DRY SAND

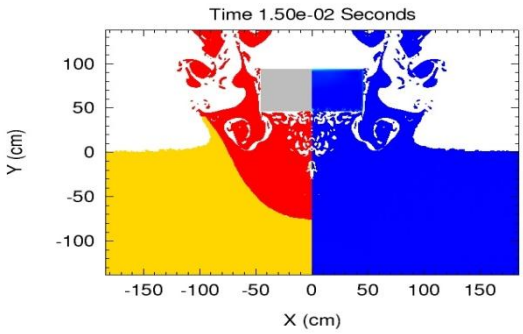

2.16b) IMD INT SOIL

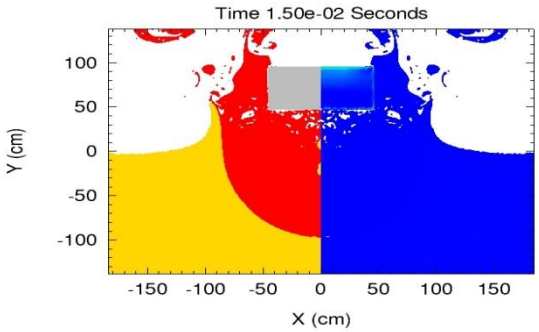

2.16c) IMD WET CLAY

Figure 2. 16: Material plots at 15ms for three IMD soils showing crater geometry

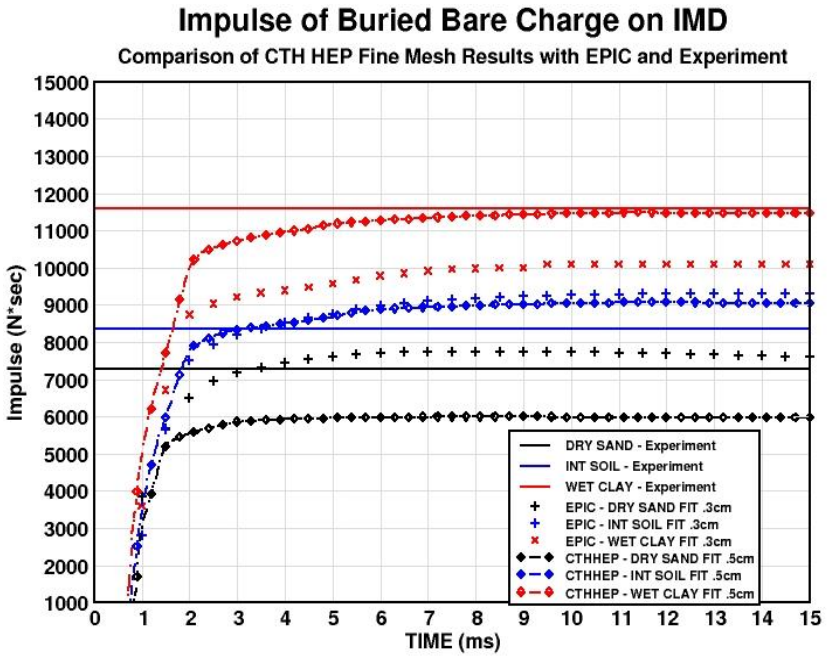

Figure 2. 17: Correlation of CTH HEP and EPIC impulse on IMD with experiment for refined mesh

2.4.6 Effect of material strength on impulse and crater geometry: Results and Discussion

In an attempt to determine the cause of the under-prediction of the impulse for the dry sand case, a series of runs were made in which the HEP strength model was bypassed. The computed values of impulse for CTH HEP with and without strength are shown in Figure 2.18. There is a slight movement upward toward the experimental values for the wet soil. The intermediate soil results move upward by a large amount. For the dry sand case, the absence of material strength moves the CTH results closer to the EPIC 3 mm predictions. The large changes in the intermediate soil and dry sand results indicate the importance of the material strength model in these shallow buried simulations. Another example of this is seen in the material plot for dry sand without the material strength shown in Figure 2.19. The crater dimensions are totally erroneous. The dry sand results confirm that a better implementation of the HEP strength model is needed along with a better procedure for defining material failure and fracture. It should be noted that these results were generated using different values for MMP (MMP3) and PFRAC (principle stress form) due to some stability problems encountered so the values with strength will differ slightly from the previous results. The effects of these parameters are described in the next section.

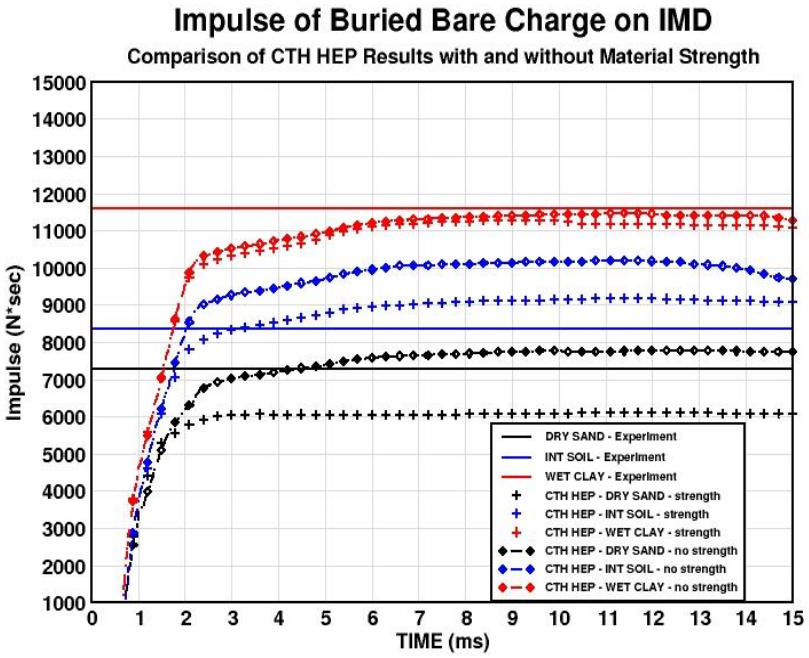

Figure 2. 18: Effect of material strength on impulse on IMD for CTH HEP model with and without strength

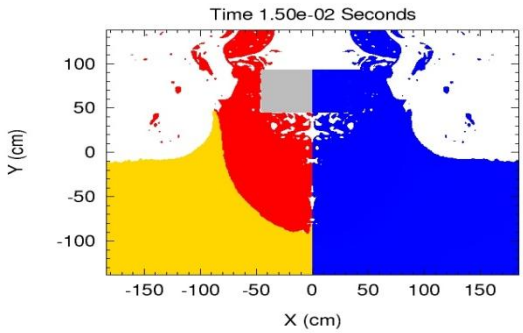

Figure 2. 19: Material response at 15 ms of IMD DRY SOIL material without strength

2.4.7 Effect of CTH MMP and PFRAC values: Results and Discussion

Figure 2.20 illustrates the effect of changing the CTH MMP and PFRAC parameters on the computed impulse. The values using the default MMP option (MMP0) with a pressure based PFRAC value of -1.E4 dynes/cm^2 are compared with results using MMP3 and a stress based PFRAC input with the principle stress for fracture assumed to be -1.E4 dynes/cm^2. The CTH MMP options determine how CTH distributes volume and energy for multi-material cells. For MMP0 this distribution is a linear function of volume fraction. MMP0 has no mechanism for relaxing pressures to an equilibrium value. By contrast, MMP3 sets a limit on the amount of PdV work that is allocated based on a cutoff value of volume fraction. In addition, pressure relaxation is allowed between materials in a cell. It can be seen that use of

MMP3 and a stress based PFRAC shifts the impulse values down with the amount of shift dependent on the material strength. This result indicates that more testing needs to be done to quantify the best combination of MMP and PFRAC for CTH HEP runs.

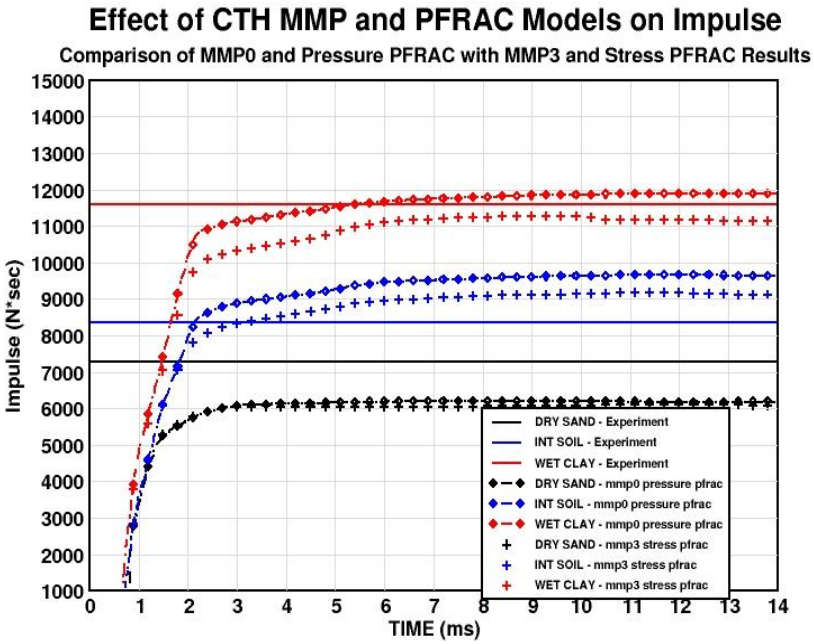

Figure 2. 20: Correlation of impulse on IMD for CTH HEP model with different values of PFRAC and MMP

2.4.8 Effect of JC Fracture model on impulse and crater dimensions: Results and Discussion

In an attempt to determine the cause of the under-prediction of the impulse for the dry sand case, a series of runs were made to evaluate methods to improve the correlation of impulse for the dry sand material. A review of the HEP model implementation in the EPIC code revealed that EPIC requires an effective strain at failure as an input. This value is used to determine when EPIC flags a material as failed and then bypasses the strength calculation for that material. A review of the strength and failure models in CTH showed that the Johnson-Cook fracture model could provide a similar capability for the HEP model if only the first of the five standard JC fracture model inputs (D1) was set to a small strain value and the spall pressure input was set to a suitable PRAC value. After a series of numerical experiments, it was determined that a D1 value of 4% with a spall pressure (PF0) of -1.0E6 showed substantial improvement in the impulse correlation with EPIC and the IMD experiments at the cost of a slightly worse prediction for the dry sand material. For the other two IMD materials, using the JC fracture model had either little or no effect for the wet clay material or slightly degraded correlations for the intermediate soil. Figure 2.21 shows the impulse correlation using the JC fracture model. Figure 2.22 shows the predicted crater dimensions for the three soils. These results illustrate the need for further research into an appropriate failure algorithm for the HEP model.

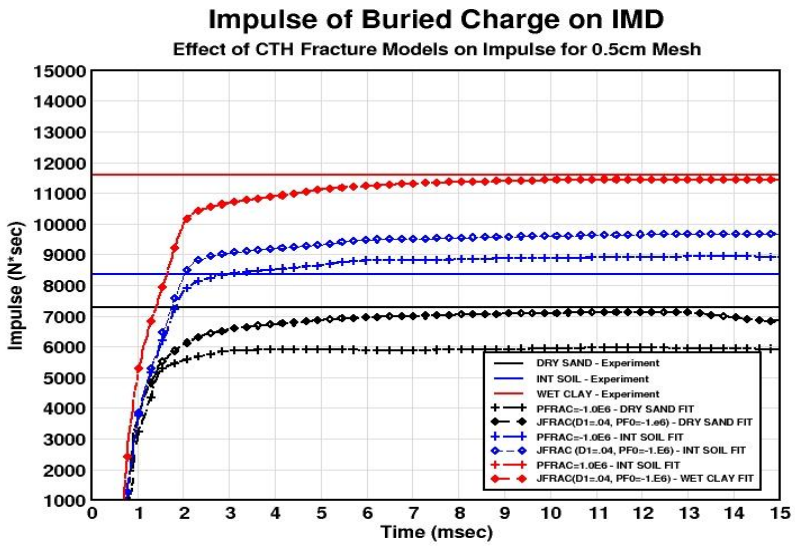

Figure 2. 21: Correlation of Impulse on IMD for CTH HEP and EPIC with experiment using JC fracture model

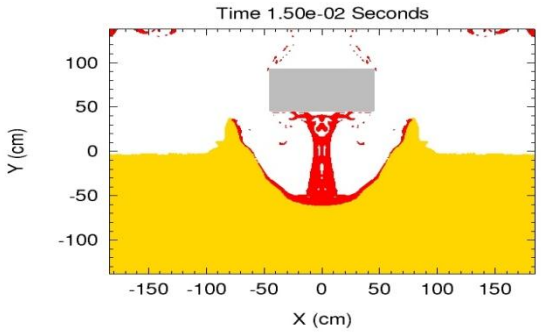

2.22a) IMD DRY SAND

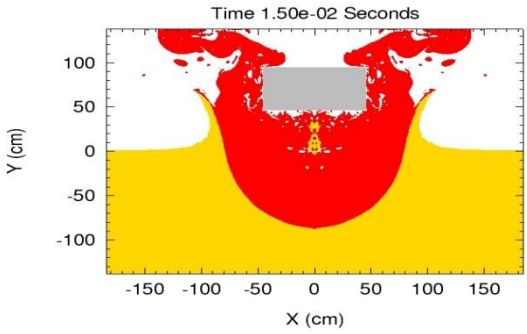

2.22b) IMD INT SOIL

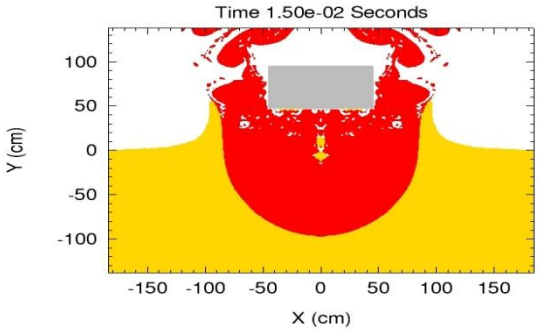

2.22c) IMD WET CLAY

Figure 2. 22: Material response at 15ms for IMD soils using CTH HEP with JC fracture model

2.4.9 Simulation of the ERDC IMD experiment with Bessette's IMD model

The IMD shallow buried explosion test for the WET CLAY material was rerun using Bessette's more detailed CTH model of the experiment. Results for impulse and material response of the soil generated by the CTH HEP model were compared with results obtained using Bessette's fit for the IMD WET CLAY material using Kerley's model. The CTH material plot of the initial material configuration of the detailed model is shown in Figure 2.23. The piston-plate assembly is shown in gray. The darker brown material is the test bed soil (WET CLAY). The lighter brown material is the *in situ* soil that is modeled as a silty clay using the Kerley model. The C4 charge shown in red was modeled using the History Variable Reactive Burn model (HVRB). The small spot of green material is a PETN booster charge that is used to initiate the detonation process for the HVRB model and is modeled using the JWL EOS. The set of material discards developed by Bessette for the Kerley model was used for both tests. The surrounding air is removed from this plot for clarity. A very fine 2D cylindrical mesh (2mm cell size) is used in the areas around the explosive, test bed soil, and IMD piston-plate assembly. Mesh stretching is used to extend the boundaries of the computational domain to appropriate distances for the selected boundary conditions. The total number of computational cells used in the simulation totaled over 7 million. The extent of the soil materials is taken to be semi-infinite. All runs were made using 192 cores on the MSU Talon cluster.

Figure 2.24 compares the impulse up to a time of 15 milliseconds generated by both the CTH HEP and Bessette's Kerley model fit with the peak impulse reported by Ehrgott. Both models are seen to provide excellent correlation with the experiment. Figures 25a-25f show the material response for both models at t=5.e-4, 2.e-3, and 15e-3 seconds. The response at 5e-4 and 2.e-3

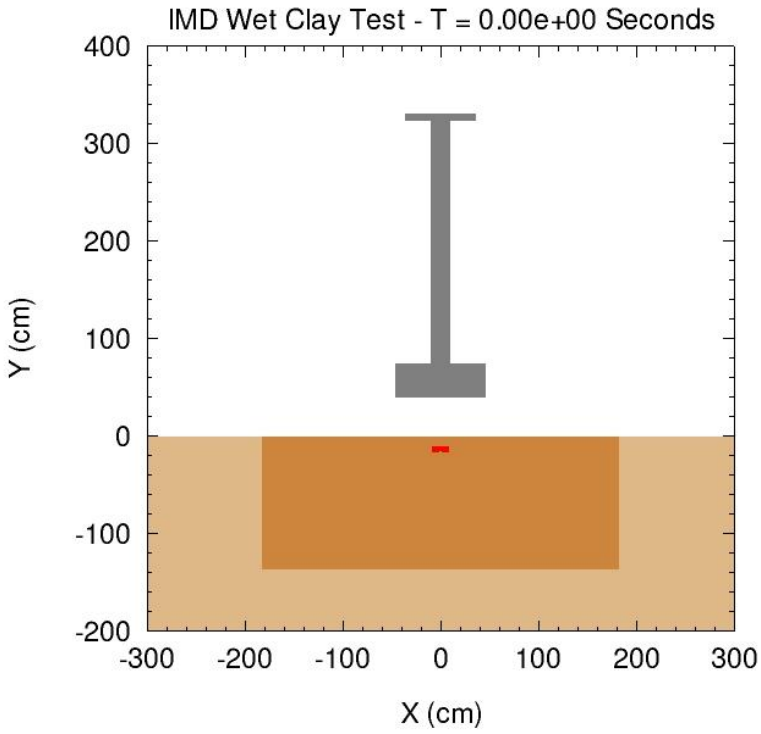

Figure 2. 23: Initial material configuration for Bessette's model of IMD experiment

seconds are very similar. The 5e-4 second shows some loss of material at the top of the soil plug being uplifted by the explosion. This loss is most likely due to the effects of the material discards used in the problem. The late time material plots show more difference than the early time plots but, as stated previously; care must be taken when trying to interpret information on crater growth from CTH material plots. One interesting aspect of these runs was the dramatic difference in run times required for each simulation. As seen in previous tests, the CTH HEP implementation was dramatically more stable requiring 83,311 cycles and 30,320 cpu seconds to reach completion compared to 229,492 cycles and 82,090 cpu seconds for the Kerley model. This difference in stability is further illustrated in Figure 2.26 that compares the stable time step computed by CTH for both models.

2.4.10 Summary of ERDC IMD simulations: Results and Discussion

The results from the ERDC IMD simulations revealed that CTH HEP provides excellent to good correlations with experiment and EPIC calculations for the wetter materials with low shear strength. The correlations are not as good as EPIC for the higher strength dry sand material. These results indicate that more work needs to be done on the CTH HEP strength model implementation and material failure models. Several options are being explored including using a CTH "modern" strength model that computes the deviatoric stresses for individual materials and implementing an effective strain failure

criterion similar to the one used in EPIC. However, it is felt that the correlations obtained for all three materials are sufficiently accurate for use in realistic simulations of shallow buried explosions.

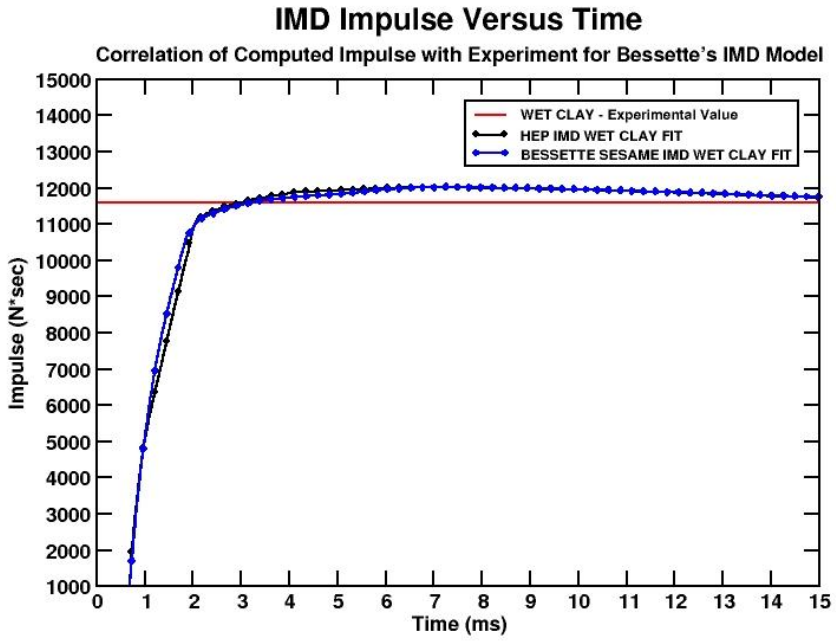

Figure 2. 24: Comparison of Computed IMD Impulse with Experiment for HEP and Bessette's fit

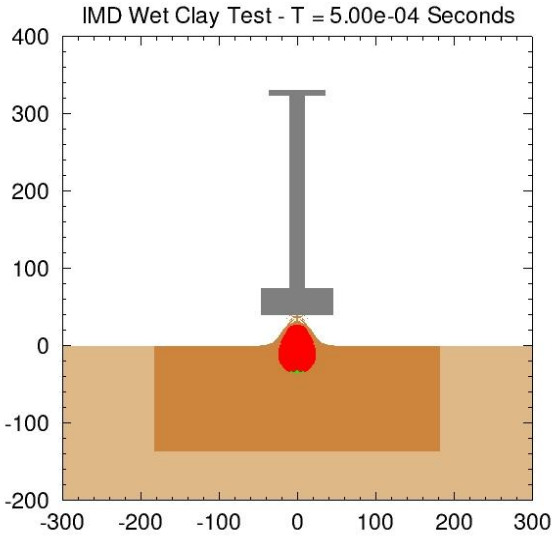

2.25a) Bessette's fit (t=5e-4s)

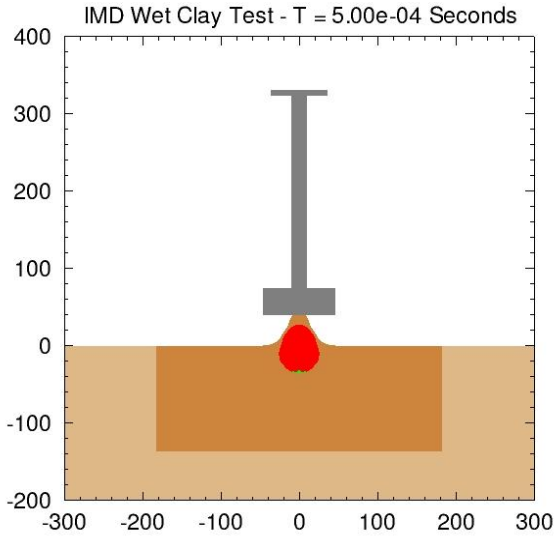

2.25b) HEP (t=5e-4s)

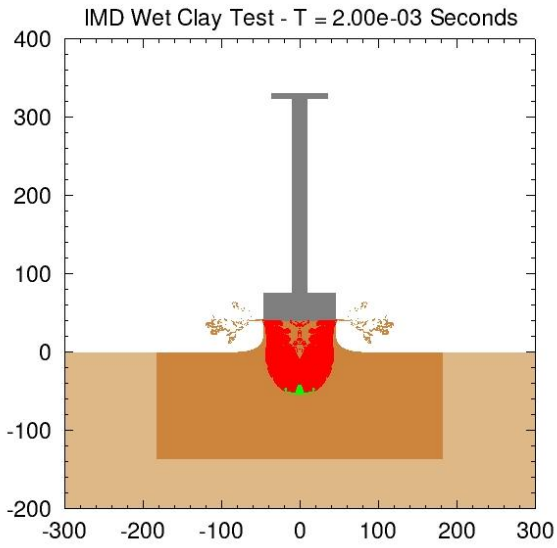

2.25c) Bessette's fit (t=2e-3s)

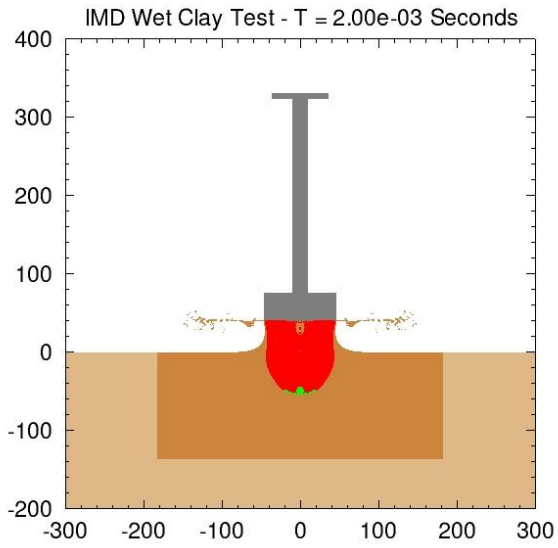

2.25d) HEP (t=2e-3s)

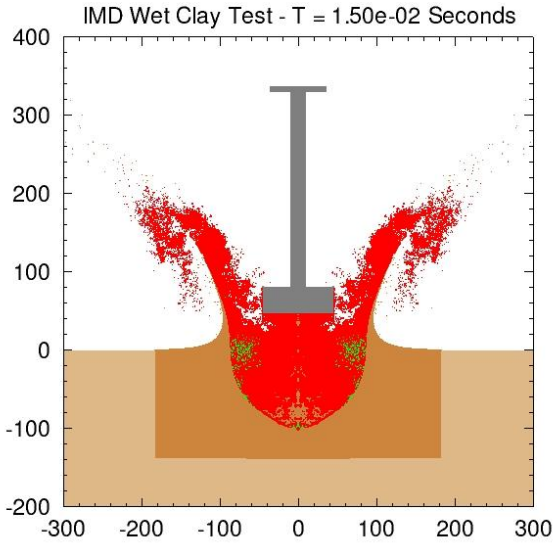

2.25e) Bessette's fit (t=15e-3s)

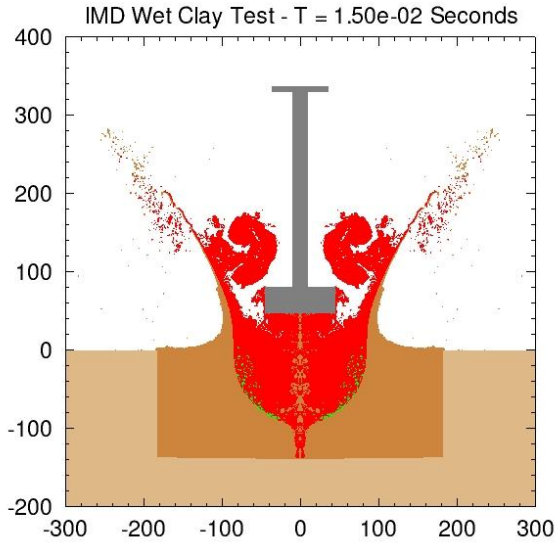

2.25f) HEP (t=15e-3s)

Figure 2. 25: Comparison of material plots for Bessette's fit and HEP at three times

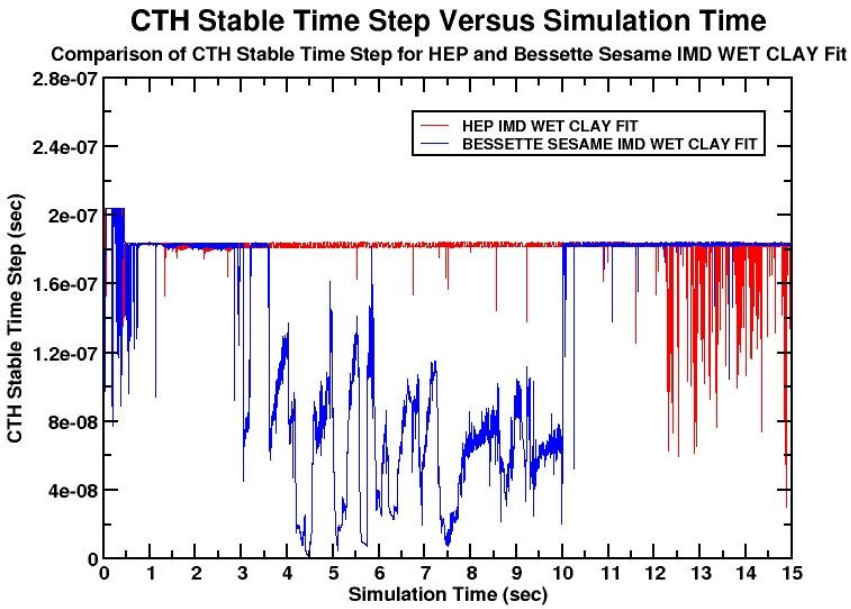

Figure 2. 26: Comparison of stable time step for HEP and Bessette WET CLAY runs

Section 3: Development of a one-way CTH to LS-DYNA coupling procedure

Over the years several researchers have attempted to provide a means of extracting results from CTH calculations for use in Lagrangian Finite Element structural dynamics codes such as LS-DYNA and DYNA3D. Of these the most successful but also the most complex, is the ZAPOTEC code from Sandia [32] that links CTH to the Sandia PRONTO3D structural dynamics code. In ZAPOTEC, the coupling is referred to as two-way, meaning that both codes run as a unit with information such as material displacement, movement of mesh nodes, and forces and moments are exchanged at either every time step or some multiple of the stable time step required by each code component. The two-way approach provides the most physically realistic simulations of Fluid Structure Interaction at a cost of code complexity and run time. An alternate approach is commonly referred to as a one-way coupling in which each code is run in separate steps with information from one code saved in a format the other code can read. The underlying assumption of the one-way coupling is that the response of the structure is much slower than the time scale of the blast or other dynamic loading event modeled by CTH. Therefore, it is assumed that extracting pressures from codes such as CTH up to a time shorter than the simulation time required to model the complete structural response and then using those pressures as time dependent loads on the structure will provide an acceptable approximation to the total force and impulse imparted to the structure at a reduce cost when compared with the two-way approach. Another underlying assumption that is common to most one-way couplers is that the material to be loaded can be considered a rigid material in the code (CTH in this case) that generates the pressures used by the structural dynamics code. The one-way coupling approach is the one selected for the current work although it might be more accurate to refer to the procedure developed as a load-curve extractor. The following sections describe the implementation of a one-way coupler between CTH and the LS-DYNA structural dynamics code and the testing done to verify the method.

3.1 Approach

The approach taken in the current CTH-LS-DYNA coupler takes its inspiration (and some of its code) from a previous one-way coupler developed by Dr. David Littlefield (UAB) [27]. Littlefield's approach allowed users to define the information required to generate load curves for LS-DYNA in standard KEYWORD format. Software embedded in CTH would then read the LS-DYNA input and generate an output file containing for load curves (DEFINE_CURVE input) in a format that could be pasted directly into the LS-DYNA inputs without modification.

Initial attempts to implement the current coupler tried to use the software developed by Littlefield for an earlier version of CTH but these proved unsuccessful due to differences in CTH 9.1 and the previous version. The primary difference was that the rigid material model developed by Littlefield that was a basic component of his coupler could not be made to work in CTH 9.1. Therefore, it was decided to keep some of the basic components of Littlefield's coupler but replace his rigid material model with the native rigid CTH rigid material model. An initial implementation was developed that assumed the elements in the LS-DYNA model were solid elements since Littlefield's coupler only supported solid

elements. As work on this task progressed, it became apparent that Littlefield's software would have to be extended to allow users to use shell elements in their LS-DYNA models. This requirement led to a complete rewrite of most of the existing Littlefield software. A description of the new and modified routines that make up the coupler is given in Appendix B.

A second major difference in the current implementation and the Littlefield implementation is the use of a time-average pressure based on an approximation of the impulse delivered to the rigid target material instead of the instantaneous pressure. The initial implementation of the coupler used the instantaneous pressure approach and it appears to yield satisfactory results for many cases. However, the time average approach is the one used in a one-way coupler between CTH and the PRESTO structural dynamics component of the Sandia SIERRA framework [28]. A careful review of the inner workings of the CTH rigid material model revealed that the time-averaged pressure approach is the one used in CTH to apply forces on a rigid material. Subsequent testing of the time-averaged approach using the DRDC plate experiment to be described later showed improved results over the instantaneous pressure approach.

The basic steps required for a coupled analysis are defined in the next section.

3.1.1 Steps required for a typical CTH-LS-DYNA coupled analysis

A coupled analysis using CTH and LS-DYNA typically involves the following steps:

1. An LS-DYNA model is generated and the surfaces to be loaded by CTH are defined by LS-DYNA LOAD_SEGMENT or LOAD_SHELL inputs. An LS-DYNA keyword input file containing the LOAD_SEGMENT or LOAD_SHELL input along with the NODE and ELEMENT input that correspond to the LOAD input needs to be created to use as input to the CTH coupler

2. If the geometry of the LS-DYNA model cannot be replicated using the native CTH material insertion facility (called diatom), the LS-DYNA model should be exported using a preprocessor such as the LS-DYNA LS-PREPOST as a Stereo Lithography (STL) format file. Note the geometry exported only needs to be the surfaces that will be exposed to the CTH generated loads.

3. A CTH input file is created for the loading side of the problem. It should contain a representation of the target geometry and inputs in a new CTH input block (delimited by a fem and endfem statement) to define the input LS-DYNA keyword file, output file that will contain the appropriate DEFINE_CURVE corresponding to each LOAD_SEGMENT or LOAD_SHELL input, and other inputs such as the frequency that the load curves are dumped to the output file.

4. CTH is run for a predefined simulation time to generate the load curve output file. This load curve file is then pasted into the LS-DYNA input files (usually as an LS-DYNA *INCLUDE file)

5. The final step is to run the LS-DYNA simulation

A more detailed description of the coupler is given in the User's Manual that accompanies the release of the enhanced version of CTH 9.1.

3.1.2 Initial implementation tests

Some initial test of the CTH component of the coupler were run to verify the software that read the LS-DYNA input files, to examine the accuracy of the procedure used to extract the instantaneous pressures used in the initial coupler implementation and to test the parallel implementation of the software. The implementation of the new coupling software in CTH 9.1 was initially verified using two test cases: an explosively loaded rigid witness plate and an example LSDYNA case that models blast loads on a cartoon "car". The rigid plate case was run in both serial and parallel modes. The load-blast-car case was run in parallel only due to the size of the grid required to contain the car geometry. Both cases are described in the following sections. The results presented used the instantaneous pressure instead of the time- averaged pressures used in the final implementation of the coupler.

3.1.2.2 Rigid plate case: Results and Discussion

The modifications to CTH 9.1 were first verified using a simple test case that consisted of an explosively loaded plate. The plate is 10 cm high, 10 cm wide and 1 cm thick. The plate is loaded by a spherical charge of TNT with a radius of 7 cm. This results in a charge mass of about 2.3 kg which is equivalent to a charge weight of about 5 lbf. The standoff distance of the plate from the center of the TNT sphere is 10 cm. The CTH programmed burn model and the JWL equation of state (EOS) for TNT are used to model the explosive. The surrounding air is modeled using the SESAME tabular EOS for air. The plate is considered a rigid material. The CTH mesh contained 80x80x80 cells with a constant 0.25 cm mesh spacing in all directions. The Z=0 and X=0 planes are specified to be a reflective boundaries. The other boundaries are specified to represent a semi-infinite medium. The simulation time for this case was 3.E-4 seconds. This test case was run in both serial and parallel mode on a Linux workstation with 6 core AMD X86-64 processor. CTH was compiled with version 11 of the Intel Fortran and C compilers. OpenMPI was used for the MPI libraries. The parallel runs used 6 cores. A material plot showing the initial configuration of the materials is shown in Figure 3.1. A contour plot of pressure at 2.e-5 seconds is shown in Figure 3.2. The spherical blast front is seen to impact along the length of the plate with the outer parts of the front wrapping around the sides of the plate and reflecting on the symmetry plane. The plate is clearly seen to be non-responding indicating that CTH is treating the plate material as rigid.

The LS-DYNA LSPREPOST tool was used to create an initial LS-DYNA model for the plate. The LS-DYNA mesh for the plate consists of 10x10x10 hexahedral solid elements with 1331 nodes. Each cell face on the Z=10 surface is specified to be a LOAD_SEGMENT. The keyword input file generated by LSPREPOST for the plate model was used as the input file for the coupling algorithm. Therefore, there will be one hundred load curves in the resulting coupling output file. The pressure time histories extracted by the coupling procedure were compared with CTH tracer data for the tracer locations that corresponded to the LOAD_SEGMENT surface centroids as well as tracers at cell centers in the cell closest to the LOAD_SEGMENT location at the LOAD_SEGMENT locations shown in Figure 3.3. For the given CTH mesh configuration, the LOAD_SEGMENT surface (Z=10) lies on a cell face. By default, CTH will try to interpolate the cell center data to the cell face. For the rigid material, this lead to the discrepancy in the extracted load curve and the interpolated data shown in Figure 3.4. The extracted curve peak is almost exactly twice the peak for interpolated tracer data. In trying to reconcile this discrepancy, it was

determine that CTH sets the pressure inside a rigid material to zero. Therefore , a simple average of the cell values on either side of the rigid surface would lead to an interpolated value of exactly one half of the value of pressure at the first cell center below the surface. The almost exact correlation between the extracted data and tracer data at the corresponding cell center shows that the pressure extraction method for the rigid material is using the first cell center off of the surface. Correlations at the other three LOAD_SEGMENT locations shown in Figure 3.5a-3.5c verify this. Figure 3.6 compares the extracted load curve data for the serial and parallel runs at the center of the plate. The correlation indicates that the parallel version of the code is generating the same results as the serial version.

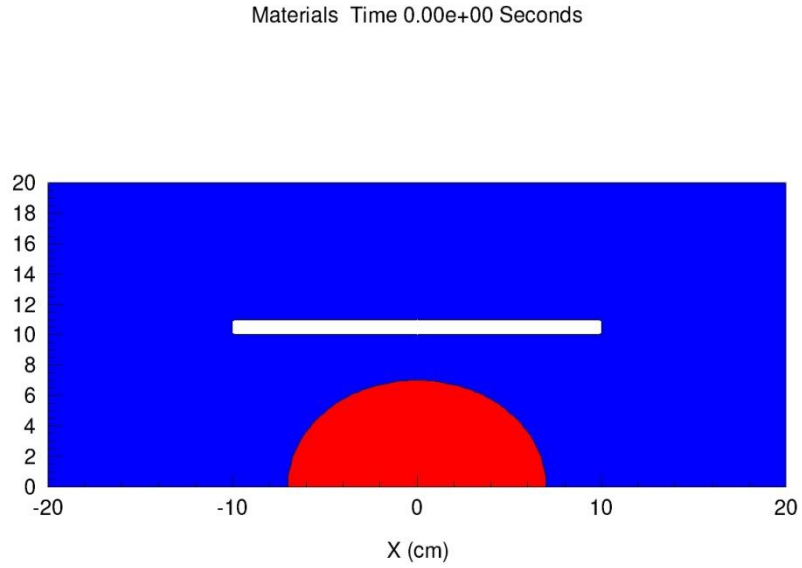

Figure 3. 1: Initial material configuration for rigid plate test

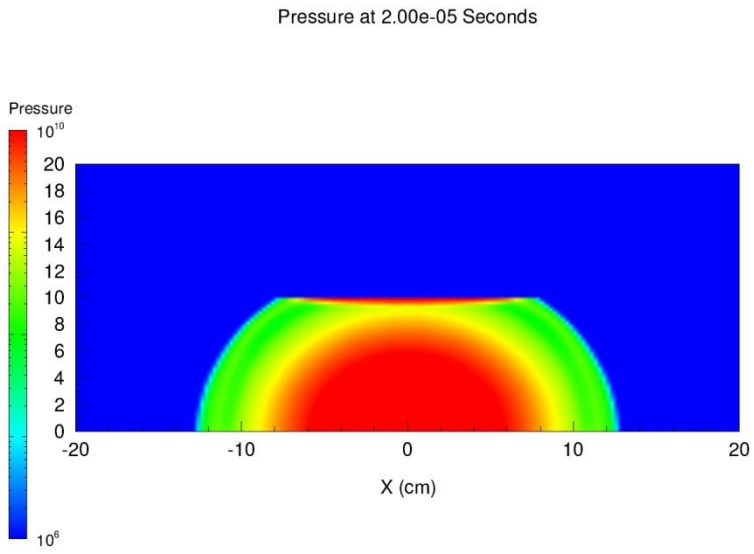

Figure 3. 2: Rigid plate pressure contours at t=2.e-5 seconds

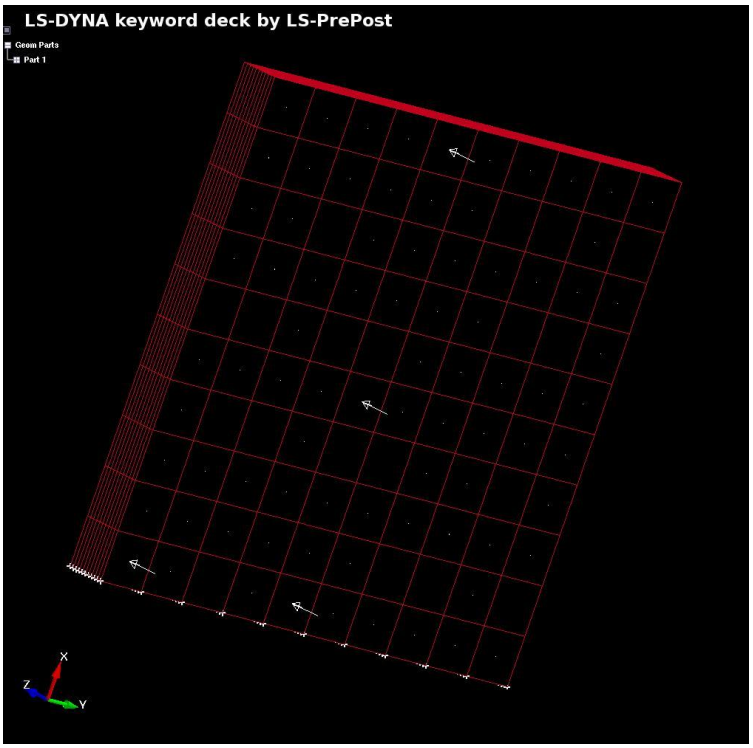

Figure 3. 3: LOAD_SEGMENT locations used in pressure correlations

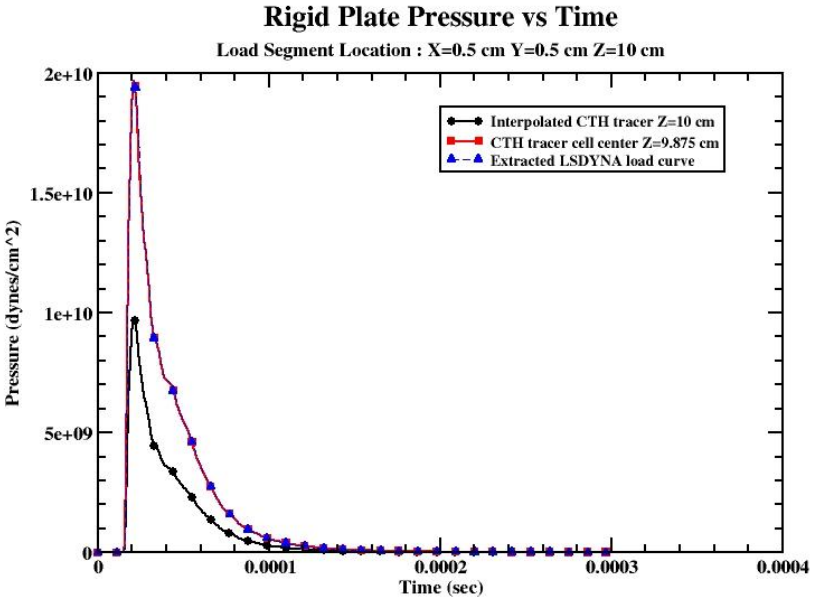

Figure 3. 4: Comparison of interpolated and extracted pressures with cell center data

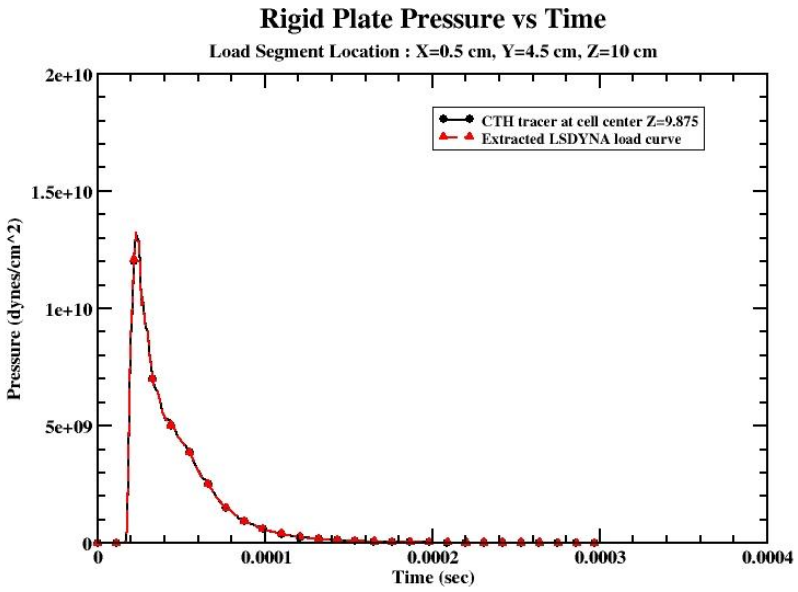

3.5a) Pressures at X=0.5, Y=4.5

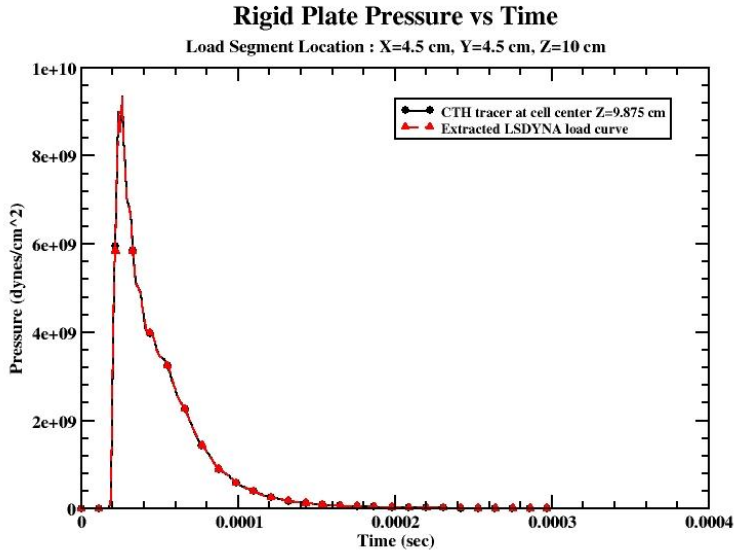

3.5b) Pressures at X=4.5, Y=4.5

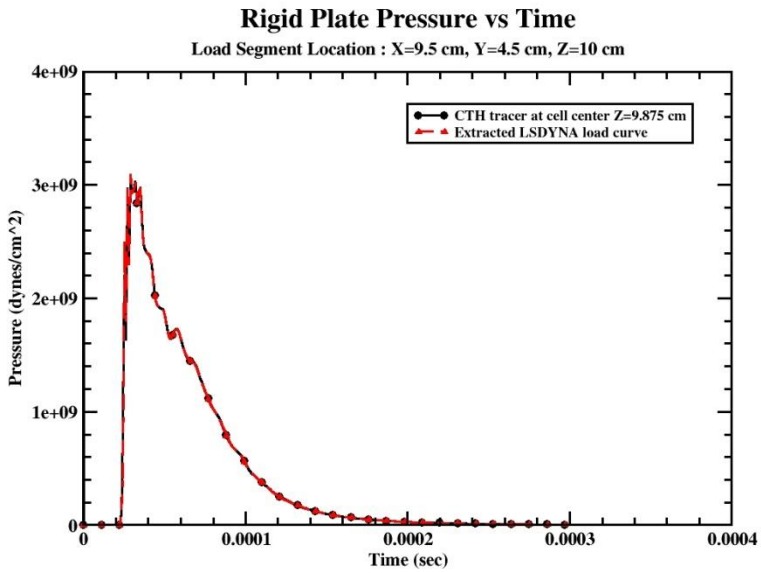

3.5a) Pressures at X=9.5, Y=4.5

Figure 3. 5: Comparison of extracted pressures will cell center pressures at 3 X locations

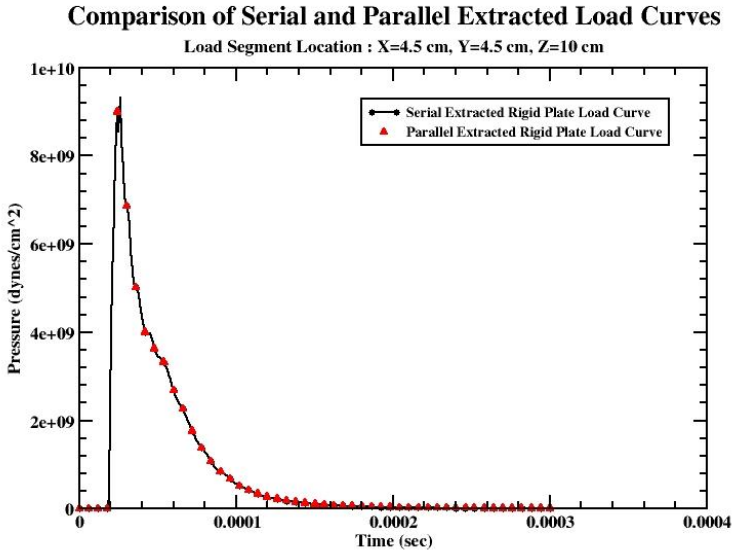

Figure 3. 6: Comparison of serial and parallel simulation pressures

3.1.2.3 LOAD-BLAST-CAR case: Results and Discussion

In order to validate the coupling procedure for a large scale problem and to verify that STL input can be used to define a rigid material in CTH 9.1, a test case based on the "cartoon" automobile geometry described in the first quarter report was constructed. The geometry and corresponding LS-DYNA keyword input file was taken from a standard LS-DYNA example problem (load-blast-car.k) used to illustrate the use of the LS-DYNA LOAD_BLAST facility. The input was modified to express the geometry in CTH units (cm versus m) and to swap the Y and Z axis to be consistent with the preferred coordinate system for 3D calculations in CTH (Z axis is up and Y is spanwise). The LSDYNA generated STL file is shown in Figure 3.7 for the initial geometry with the "tires" removed. The modified geometry was used in LSPREPOST to generate LOAD_SEGMENT input at the 36 face segments shown in Figure 3.8a.

A CTH input deck was constructed that consisted of a large mesh (900cm x 400 cm x 524 cm) with 2 cm mesh spacing in all directions. This leads to a mesh with 450 x 200 x 262 interior cells. The Z=-24 plane is taken as a reflecting boundary. All other exterior boundaries are set to model a semi-infinite domain. Although the mesh is large, the 2 cm spacing is not fine enough in the region of the explosive to capture the generated blast wave accurately. However, it is sufficient for the objectives of this case; mainly, to verify the coupling algorithm for a large scale case and demonstrate the use of the STL geometry from LSPREPOST to define the rigid material in CTH. The explosive charge consisted of a sphere of about 100 kg of TNT. The diameter of the sphere is 48 cm. The detonation point of the explosive was at X=340, Y=100, Z=-24.0 which is just in front of the left front "tire" of the car. The explosive was modeled using the JWL equation of state. Simulations were run on in parallel using 60 processors on the MSU HPCC Talon cluster. Pressure time histories were saved and extracted every microsecond.

A material plot for a 2D sections of the grid in the Y=0 cm symmetry plane at 2.8e-4 seconds is shown in Figures 3.9. This plot illustrates the ability of the CTH STL input option to preserve the key features of the geometry when it is inserted into a 3D Cartesian mesh.

Results comparing extracted pressure time histories versus data at CTH tracer locations are presented for the six stations shown in Figure 3.8b. These results are shown in Figure 3.10a-3.10e. Figure 3.10a again shows the discrepancy between interpolated and cell center data. However, the other plots in Figure 3.9 show a near exact correlation between the extracted values and the values for tracers defined at the cell center closest to the corresponding LOAD_SEGMENT location.

These results indicate that the coupling algorithm and STL geometry definition procedure works for a realistic large-scale simulation. In particular, the baseline coupling algorithm is shown to work with the default CTH rigid material model.

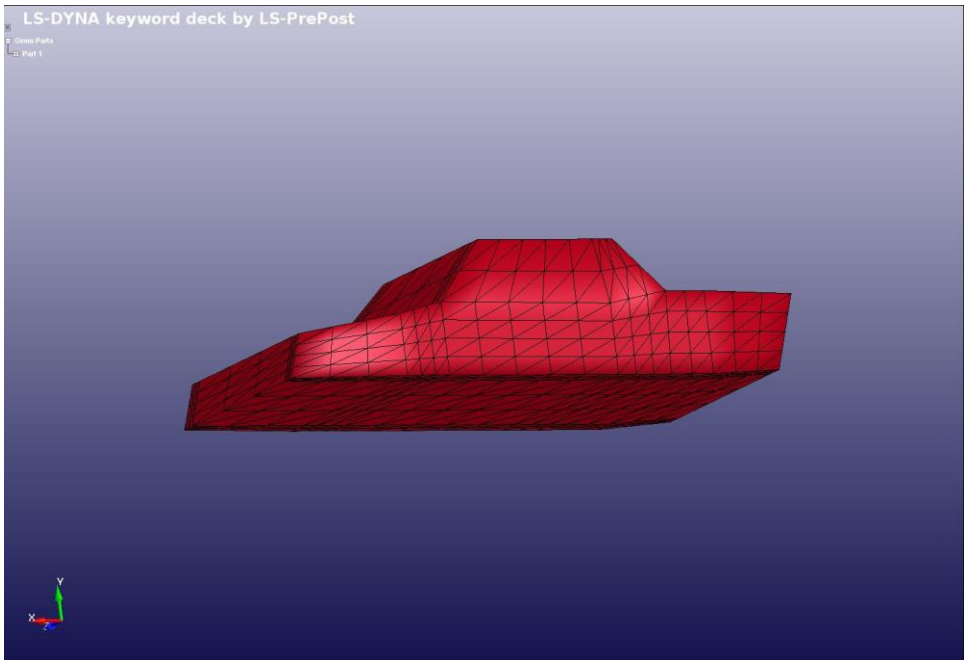

Figure 3. 7: STL Representation of cartoon car

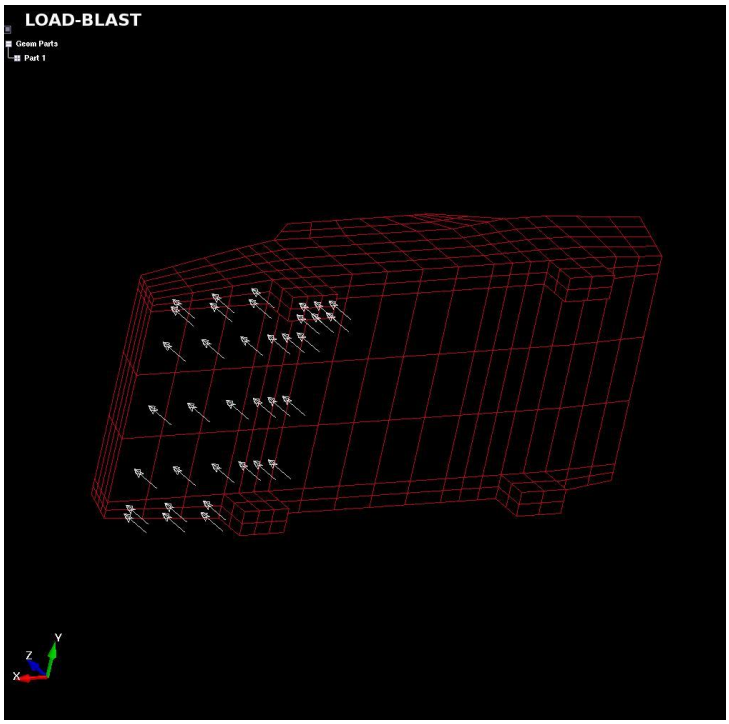

3.8a) LOAD_SEGMENT elements defined for cartoon car

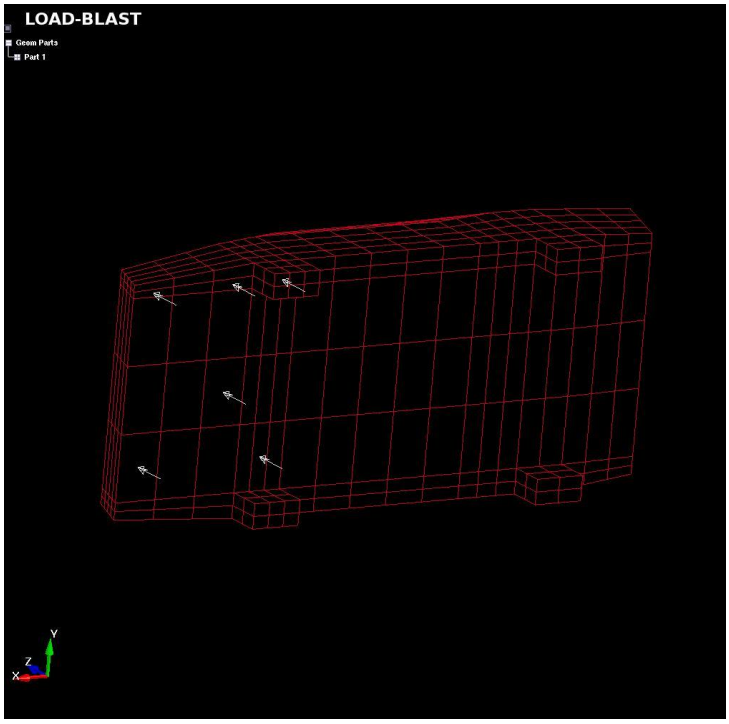

3.8b) LOAD_SEGMENT locations used in pressure correlations

Figure 3. 8: LOAD_SEGMENT elements

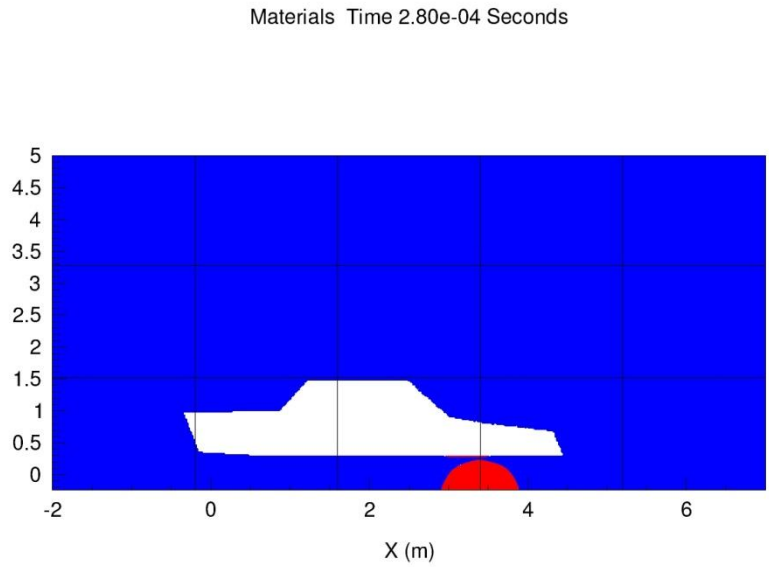

Figure 3. 9: Material plot in Y=0 plane at 2.8e-4 seconds

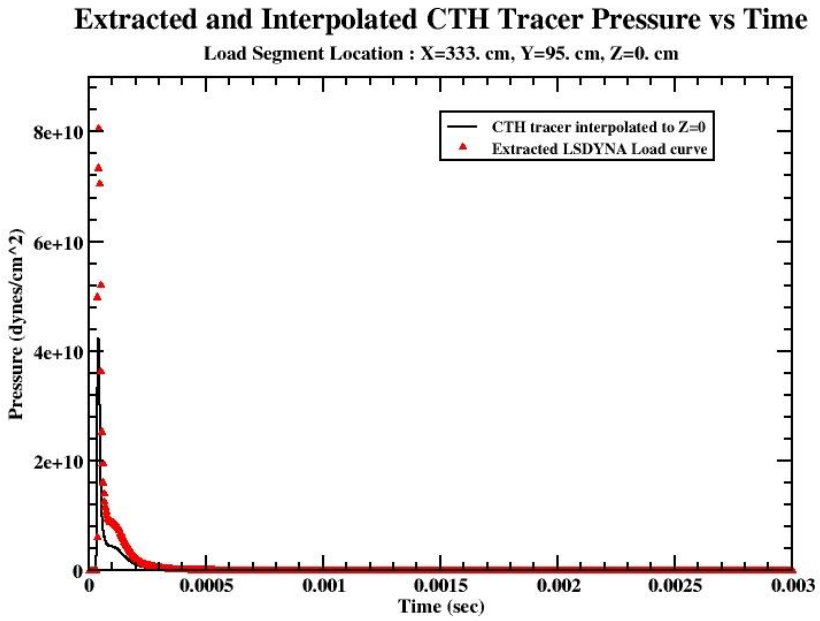

3.10a) Pressures at X=333, Y=95, Z=0

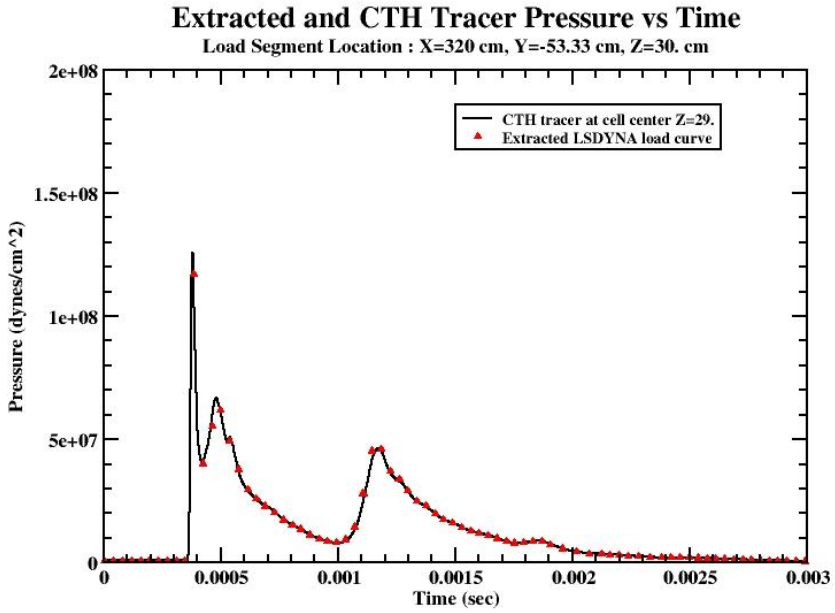

3.10b) Pressures at X=320, Y=-53, Z=30

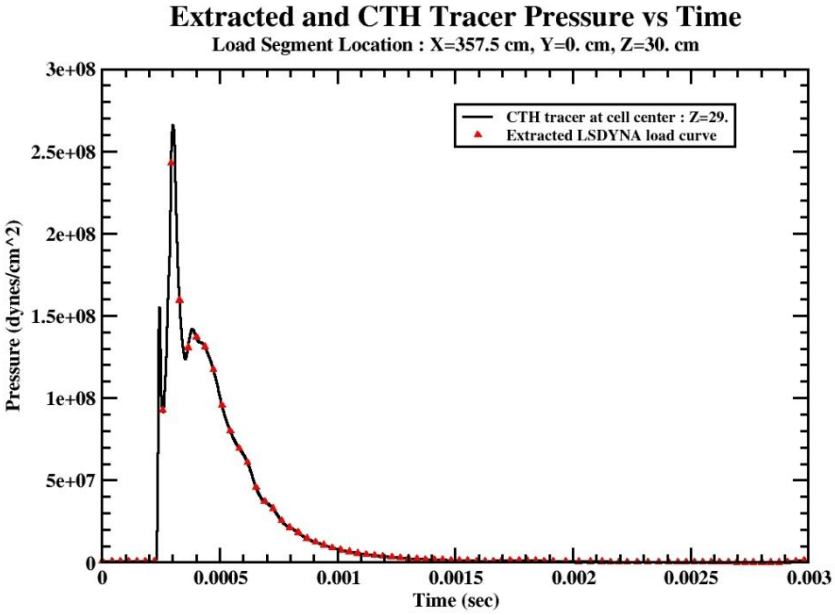

3.10c) Pressures at X=357.5, Y=0, Z=30

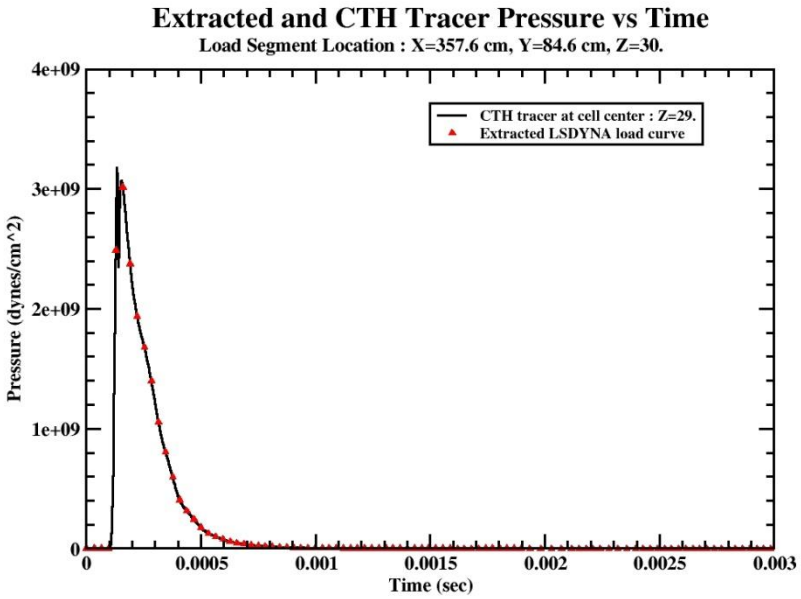

3.10d) Pressures at X=357.6, Y=84.6, Z=30

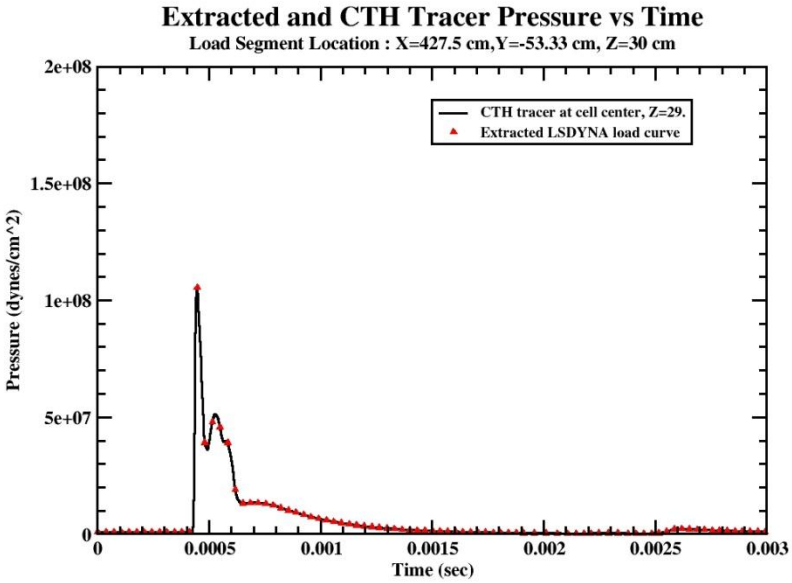

3.10e) Pressures at X=427.5, Y=-53.33, Z=30

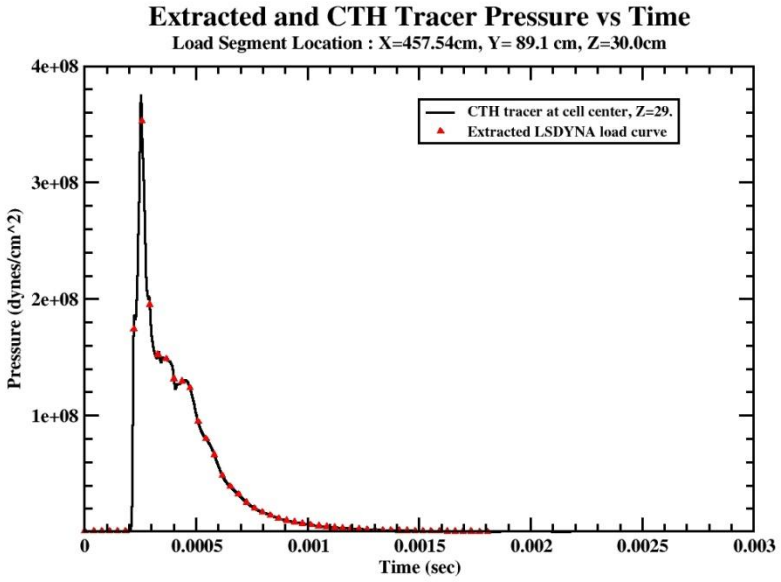

3.10f) Pressures at X=457.54, Y=89.1, Z=30

Figure 3. 10: Comparison of extracted pressures and cell center pressures at 6 locations

3.2 Full scale tests of the one-way coupler

A full scale test of the coupler was delayed by implementation of the HEP model. When testing resumed, it focused on two test cases. At the suggestion of TARDEC/CASSI Analytics, the first full scale test of the CTH – LS-DYNA coupler attempted to simulate results for the DRDC plate experiment [24]. A second full scale test attempted to model the Generic Hull experiment used in validating the Loci-Blast/LS-DYNA coupler developed in SimBRS WD0034 [29]. The DRDC plate experiment has been subjected to a variety of analyses over the last several years including use of LS-DYNA ALE, LS-DYNA SPH and FEM coupling, and PAM-SHOCK SPH-FEM coupling [30, 31]. The PAM-SHOCK SPH-FEM approach was also applied to the Generic Hull experiment in Reference 30. The next sections describe results from the using CTH alone and the CTH-LS-DYNA coupler to simulate the DRDC plate experiment and the CTH-LS-DYNA coupler to simulate the Generic Hull experiment.

3.2.1 Simulation of the DRDC plate experiment: Results and Discussion

LS-DYNA3D ALE and LOAD_BLAST models of the target plate and support structure geometries were provided by TARDEC and used to develop a CTH input deck. On reviewing the LS-DYNA input decks, it was found that shell elements were used in the LS-DYNA analysis. This complicated the analysis since CTH 9.1 does not handle shell elements. Plate thicknesses were added to the LS-DYNA shell element definitions to generate a 3D model of the materials inserted into the CTH mesh. For these simulations, the top plate was ignored along with the side plates used to constrain the lateral motion of the support

frame. The soil was modeled using the CTH HEP model for dry sand. The dry sand material density does not match the density of the soil used in the LS-DYNA simulations but was chosen based on the results from the ERDC IMD experiment simulations and represents a lower bound on impulse that will be applied by the soil and explosion to the target plate. The target plate used was the 5083 aluminum plate used in the LS-DYNA inputs we received from TARDEC. The plate thickness used was the experimental value of 3.175 cm. As reported in Reference 24, the explosive charge consisted of a 6 kg cylinder of C4 with a diameter of 25.4 cm and a thickness of 7.62 cm. The DOB is taken to be to the top of the charge and was set at 5 cm. The default Johnson-Cook constitutive model for 5083 aluminum was used with the individual parameters adjusted to match the LS-DYNA input values. The Johnson-Cook Fracture model was also used. The SESEME Equation of State values for 2024 aluminum with density adjusted to match the 5083 value was used for the target plate due to the lack of a default EOS model for 5083 aluminum. The SESAME EOS tables for 4340 steel were used for the EOS input and the default Johnson-Cook steel values were used for the constitutive model. The surrounding air was modeled using the SESAME EOS. Quarter symmetry was used to reduce the problem size. However, the thin plates used in the geometry require a fine mesh to resolve the material. Therefore a graded mesh using 5 mm mesh spacing in the immediate region of the test geometry and the charge was used with mesh stretching used to extend the mesh to appropriate outer boundaries. Even with a mesh grading, the resulting mesh contains 280x280x480 (37,632,000) cells. Due to the size of the grid, these simulations were run on the MSU HPCC Talon cluster using 192 cores. A diagram of the DRDC plate experiment test configuration taken from Reference 24 is shown in Figure 3.11. A 3D view of the initial CTH configuration is shown in Figure 3.12. An additional 1 metric ton of weight that sits on top of the frame is not shown. An initial set of CTH alone simulations were run prior to running the CTH-LS-DYNA coupler to examine the effect of mesh spacing on run times, the stability of the simulation using the HEP soil model, and to see how accurately CTH could model the DRDC plate response on its own.

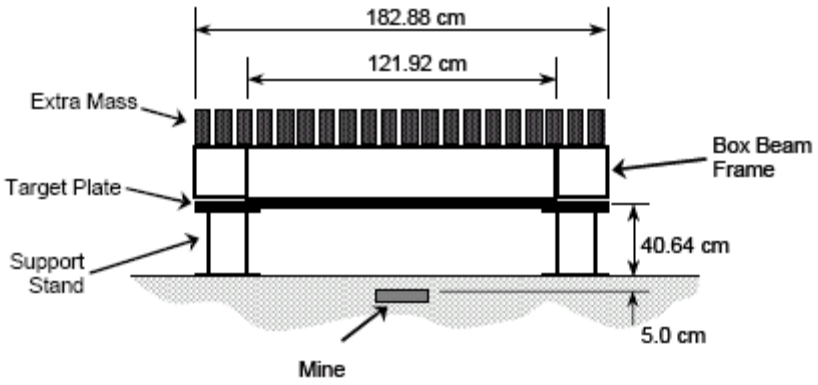

Figure 3. 11: DRDC plate experiment test configuration (Reference 24)

3.2.2 LS-DYNA ALE and CTH alone simulation of DRDC plate experiment

Prior to running the CTH simulations, the LS-DYNA input decks obtained from TARDEC were run using both the ALE and CONWEP inputs. Figure 3.13 shows the plate deformation obtained using the CONWEP based LOAD_BLAST facility in LS-DYNA to provide the blast loads to the structure. For the CONWEP case

the plate is seen to deform but not fail which matches the experiment. Next the LS-DYNA ALE case was run using the default material properties for the target plate obtained from TARDEC. With these inputs, the plate is seen in Figure 3.14 to exhibit fracture under the blast load that is not indicated in the experiment. Figure 3.15 shows the response obtained from running CTH alone using the same Johnson-Cook inputs for the plate used in the LS-DYNA ALE case. The CTH results show an even more dramatic plate fracture response than LS-DYNA. Several numerical experiments were conducted to determine the cause of the fracture. These experiments indicated that the parameters used in the Johnson-Cook Fracture model were resulting in premature failure of the plate. These parameters were modified to set the leading value (D1) to 150% and the rest of the parameters to zero. This modification was similar to that used with the JC fracture model application to the HEP soil model. The effect of this modification is to turn off all rate and thermal effects in the fracture model. Although there is no physical basis for this modification, the results presented in Figures 3.16-3.18 show that the change in fracture model inputs leads to improved prediction of the deformation response for both LS-DYNA and CTH. The material deformation responses show in Figures 3.16 and 3.17 are now consistent with the LS-DYNA CONWEP results. The plate centerline displacement time history is show in Figure 3.18 for both the LS-DYNA ALE and CTH HEP simulations. The predicted value of displacement at 6 ms compares favorably with the 300 mm value measured in the experiment. These results illustrate the importance of the fracture model in predicting plate response. Although the IMD DRY SAND material yielded surprisingly good results for the centerline displacement for the CTH alone tests, this should not be considered an indication that it is an appropriate analog for the soil used in the DRDC experiments.

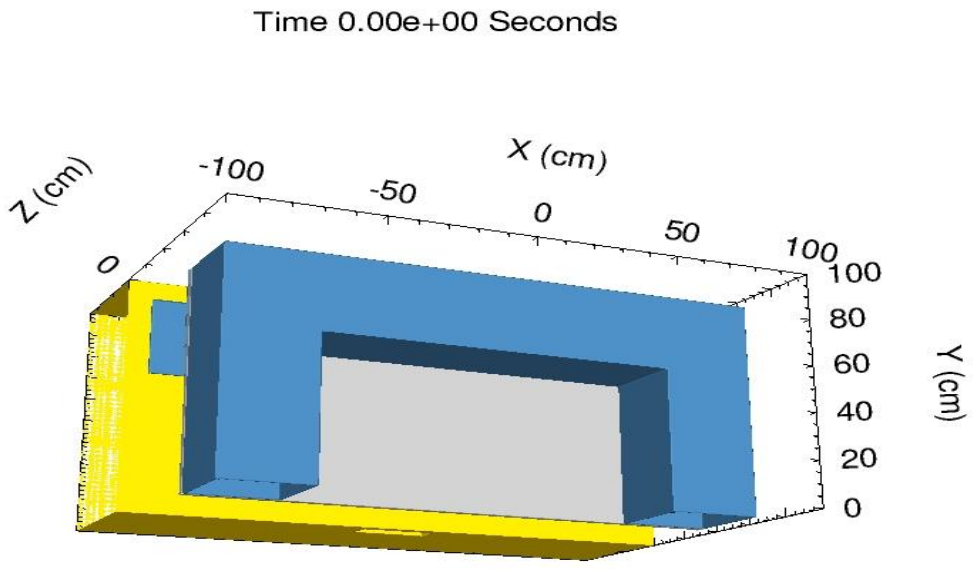

Figure 3. 12: Initial CTH material configuration for DRDC plate model

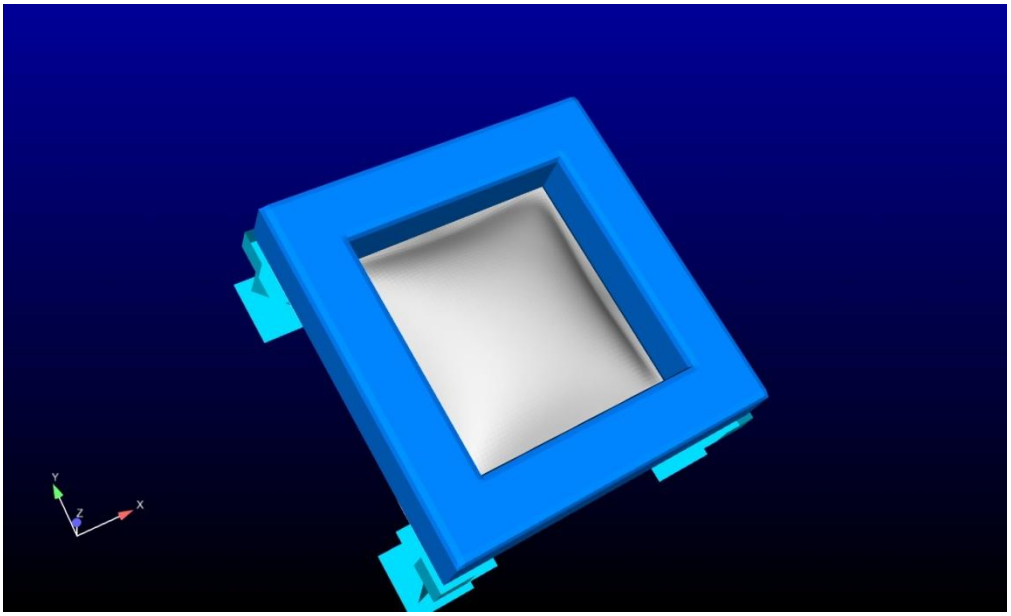

Figure 3. 13: DRDC Plate deformation for LS-DYNA LOAD_BLAST analysis

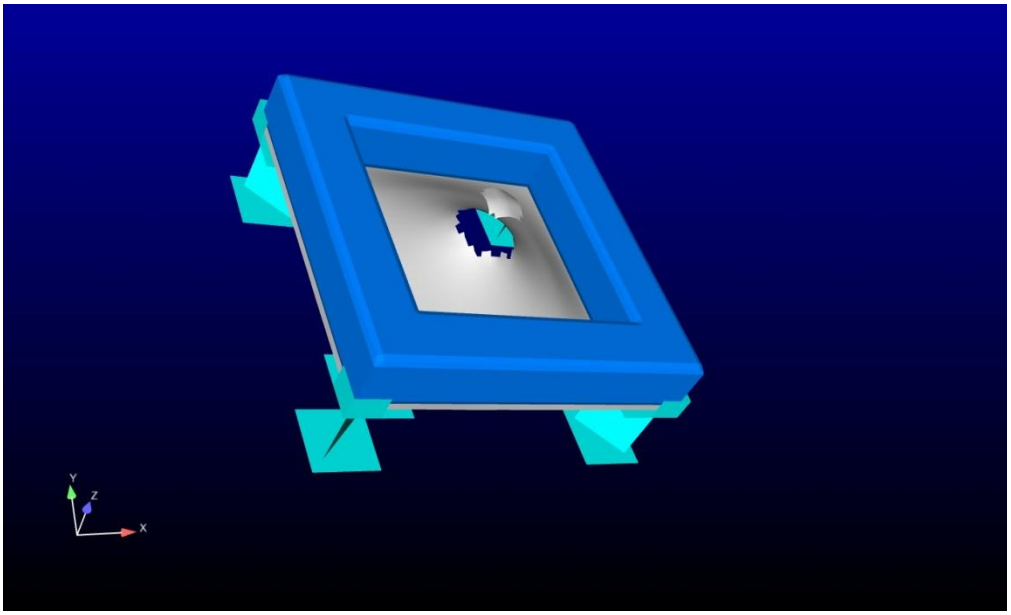

Figure 3. 14: DRDC Plate deformation for LS-DYNA ALE analysis with default JC fracture values

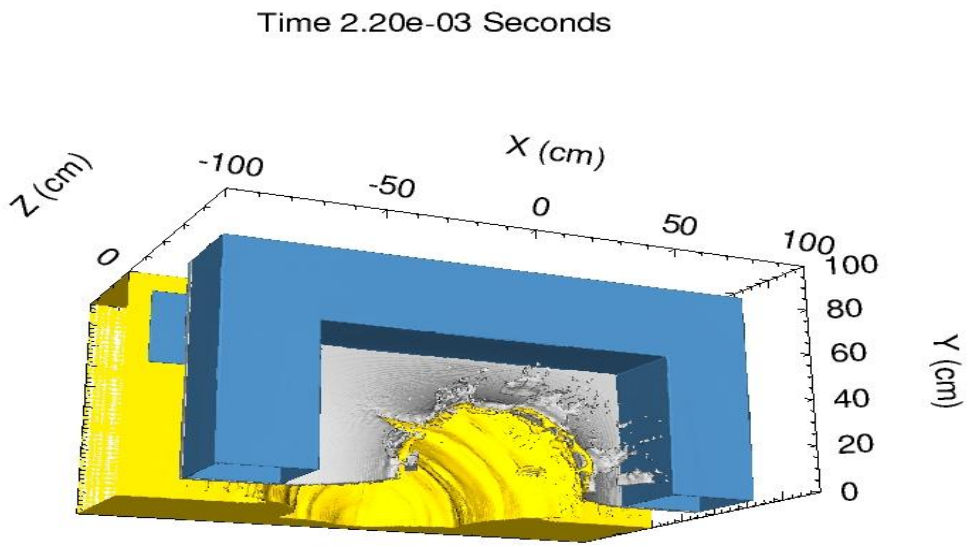

Figure 3. 15: DRDC plate deformation for CTH HEP analysis with default JC fracture values

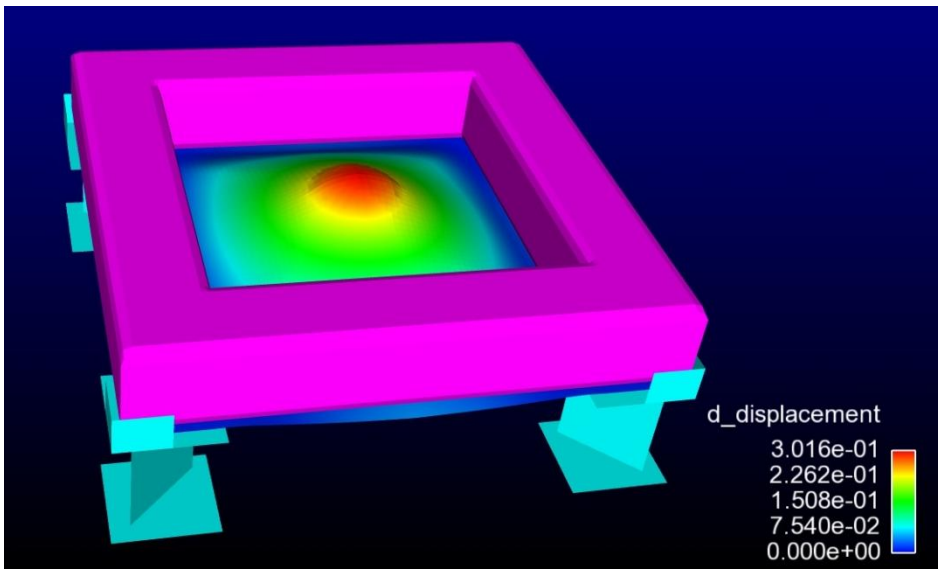

Figure 3. 16: DRDC plate deformation for LS-DYNA ALE analysis with modified JC fracture values

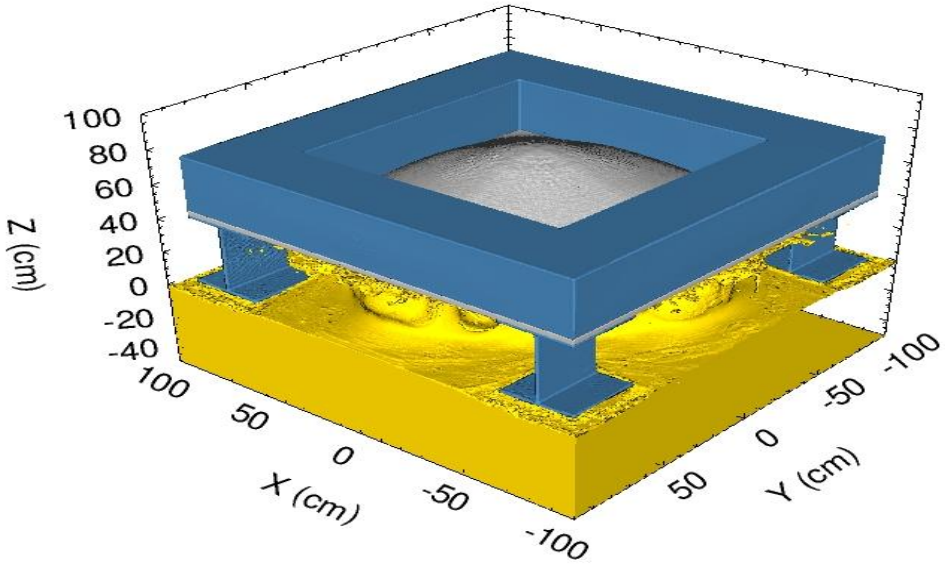

Figure 3. 17: DRDC plate deformation for CTH HEP analysis with modified JC fracture values

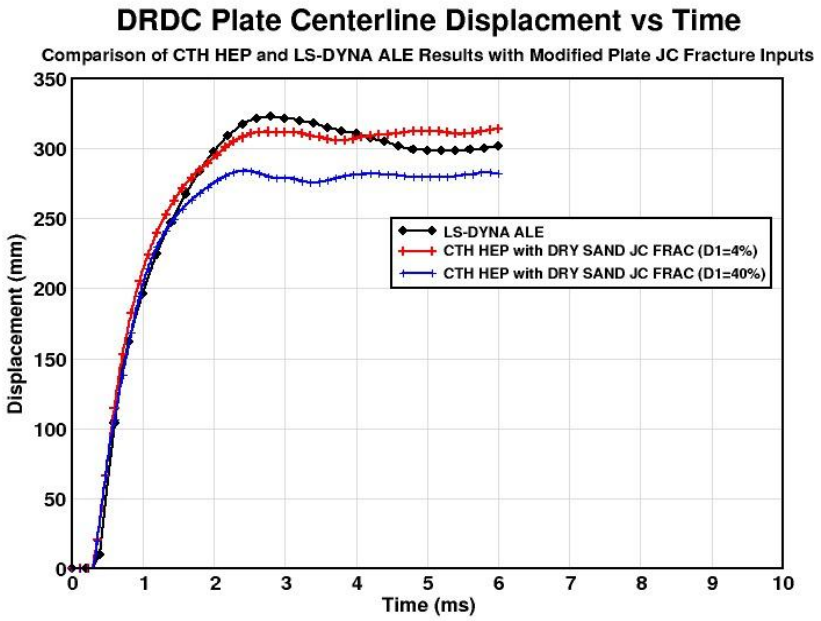

Figure 3. 18: Comparison of predicted DRDC plate centerline displacement versus time

3.2.3 CTH to LS-DYNA one-way coupling results for DRDC plate experiment

Two sets of simulations of the DRDC plate experiment were performed using the CTH/LS-DYNA coupler. In the first set of simulations, the instantaneous pressures on the plate were used to define the load curves. In the second set of simulations, the time average approach to defining the load curve pressures was used. The CTH inputs for the DRDC geometry developed for the CTH alone calculations were used with the exception that the supporting legs were removed to match the definition of the load curves generated by LS-PREPOST. The 5 mm mesh spacing used in the CTH alone case was repeated in the coupled cases. CTH simulations were first run to 5e-3 seconds and the extracted load curves were fed into an LS-DYNA simulation that ran for 8e-3 seconds. Figure 3.19 compares the displacement of the plate at element locations in the symmetry plane of the plate from the plate center to the plate edge computed using both the instantaneous and time averaged CTH pressures with experiment. It is seen that the time average results gives a much better correlation with experiment for this case. The overprediction of the deformation near the plate edge with the time-averaged pressures needs to be investigated further. A contour plot of displacement is shown in Figure 3.20.

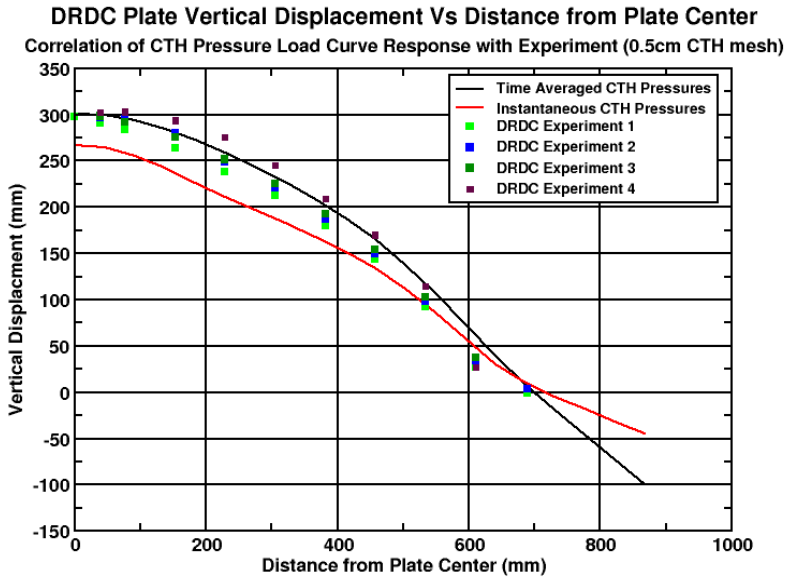

Figure 3. 19: Comparison of plate deflection using time-averaged and instantaneous CTH pressures with experiment

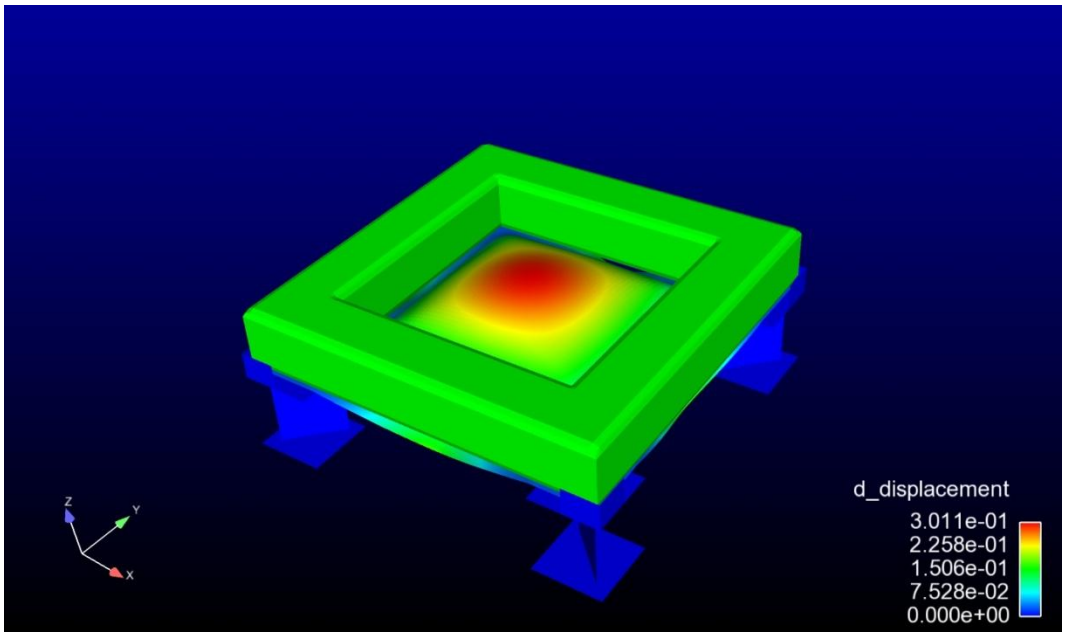

Figure 3. 20: Displacement contours using time-averaged CTH pressures

3.2.4 Simulation of Generic Hull experiment using CTH to LS-DYNA one-way coupling: Results and Discussion

The TARDEC Generic Hull experiment was designed to provide a notional geometry for underbody blast analysis and to evaluate blast mitigation technology. Historically, the Department of Army has had difficulty collaborating with industry and academia on underbody blast events due to the sensitive nature of the work. Data generated from testing military vehicles is typically rated CLASSIFIED and not readily sharable. To alleviate this issue, TARDEC has fabricated a generic vehicle hull (Figure 3.21) with the intent to share data with academia and the industry to spur innovation in blast mitigation technologies [30, 33].The availability of an existing LS-DYNA model obtained for the Loci-Blast/LS-DYNA coupling work done under SimBRS WD0034 made it an excellent choice for the final tests of the one-way coupler. As a first step in the simulation process, an STL file of the exterior of the GHULL LS-DYNA model was generated using LS-PREPOST. Figure 3.21 shows that all the details of the external geometry of the LS-DYNA model are preserved in the STL file. Next, a set of LOAD_SEGMENT elements were defined for the undersurface of the GHULL configuration. The parts of the undersurface that is loaded by CTH is shown if Figure 3.22. Due to the number of elements in the LS-DYNA model, this procedure resulted in 46,729 LOAD_SEGMENT entries. This represents an extreme test of the one-way coupling software. A CTH run was created that contained approximately 149 million cells (900x360x460 cells). The mesh spacing is a constant 1cm in all three axes. The soil was modeled using the HEP IMD_INT_SOIL material which is an intermediate silty sand with a wet density of 2.01 g/cm^3. The charge weight, depth of burial, and position under the vehicle were the same values used in the SimBRS WD0034 simulations. CTH simulations were run out to 2e-3 seconds and the load curves generated where included in an LS-DYNA simulation of the complete vehicle that ran out to 5e-3 seconds. For the CTH simulations, half-

symmetry was employed but the full geometry was used in the LS-DYNA runs. This tested a feature of the one-way coupler that allows users to input a full LS-DYNA geometry into CTH but assume half or quarter symmetry in the CTH simulation. Results from the simulation are given in Figures 3.23-3.28. Figures 3.23 and 3.24 show the displacement of the external shell at 5e-3 and 2e-3 seconds. Figure 3.25 shows the external pressures remaining on the underside of the vehicle at 5e-3 seconds. Figure 3.26 and 3.27 show the effective stress and displacement of the internal frame and false floor at 1e-3 and 5e-3 seconds. These results are similar to those obtained in WD0034. The success of this simulation demonstrates that the one-way coupler can handle complex geometries and provide acceptable accuracy for analyzing the effects of buried mines on realistic vehicle geometries.

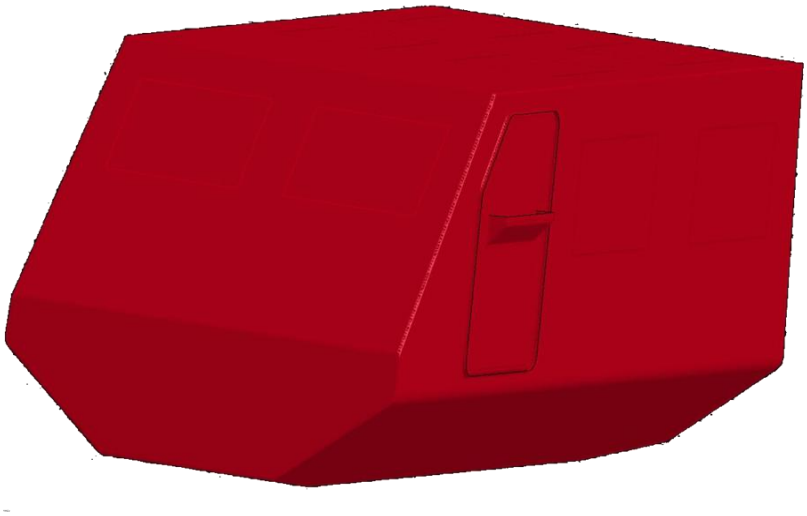

Figure 3. 21: TARDEC Generic Hull STL geometry from LS-PREPOST (above), physical hull (below)

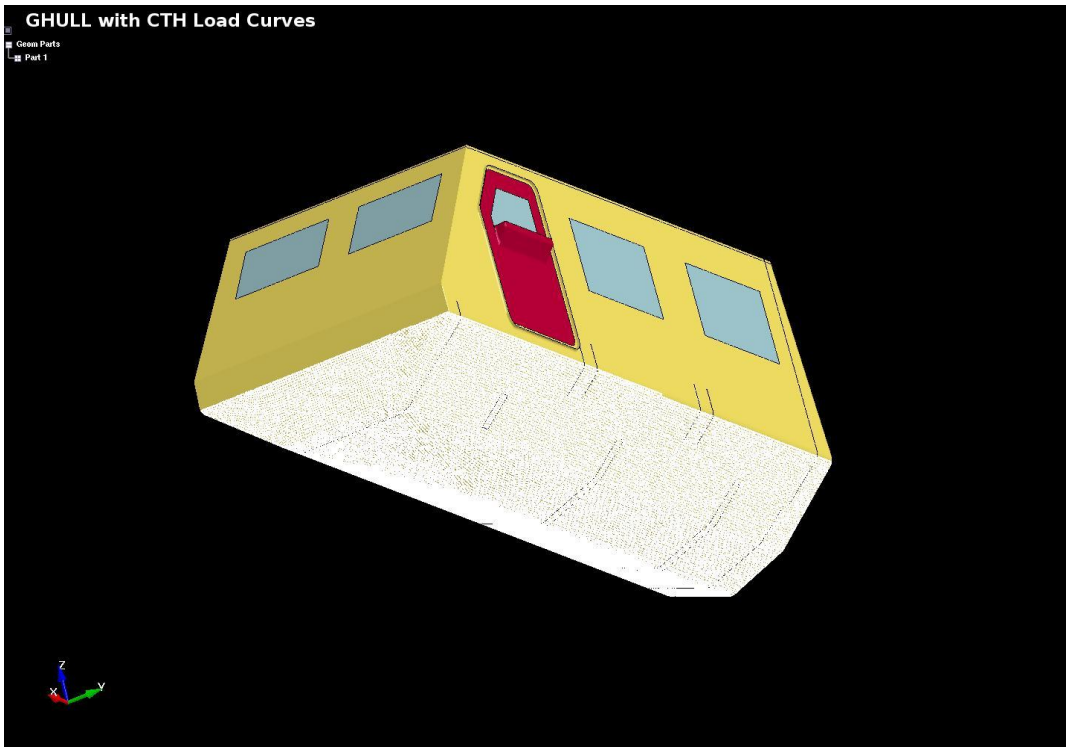

Figure 3. 22: Geometry with surfaces loaded by CTH pressures shown in white

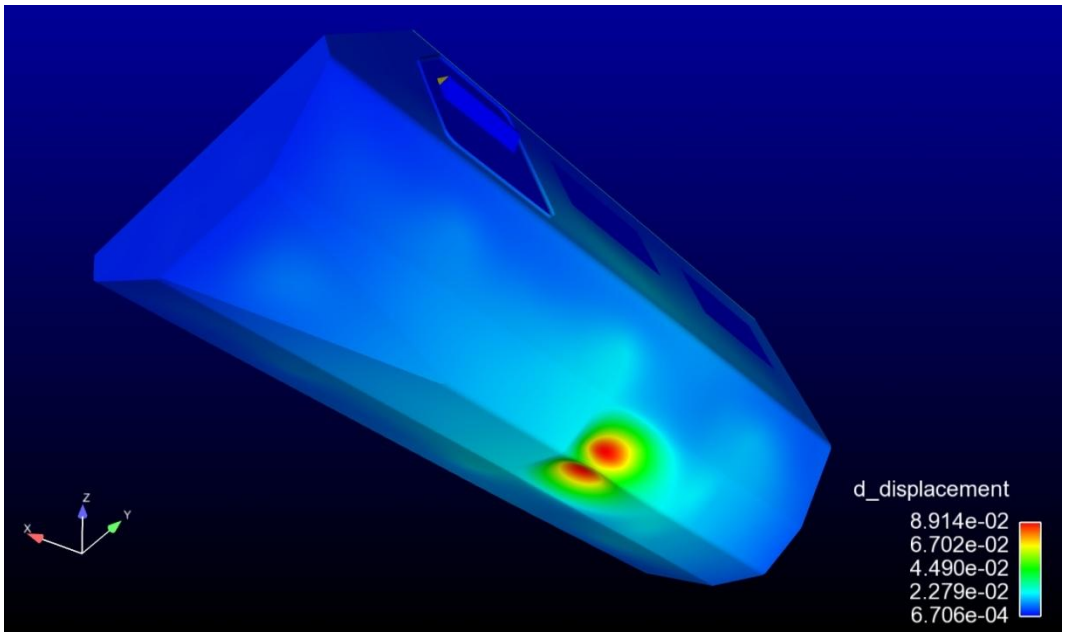

Figure 3. 23: Contours of external hull displacement at t=5e-3 seconds

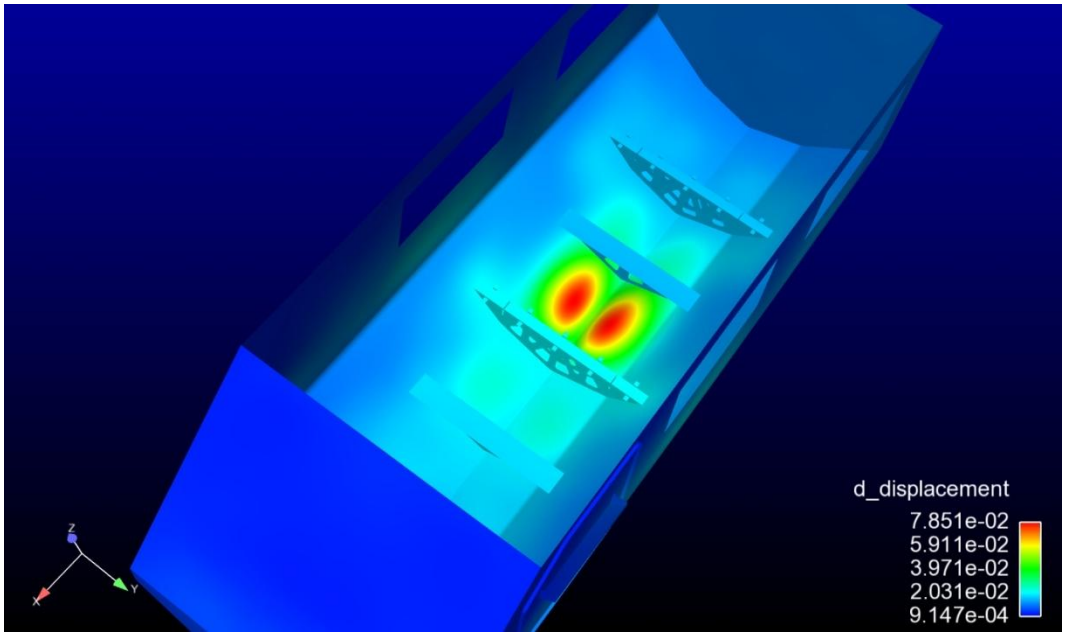

Figure 3. 24: Contours of internal hull displacement at t=2e-3 seconds

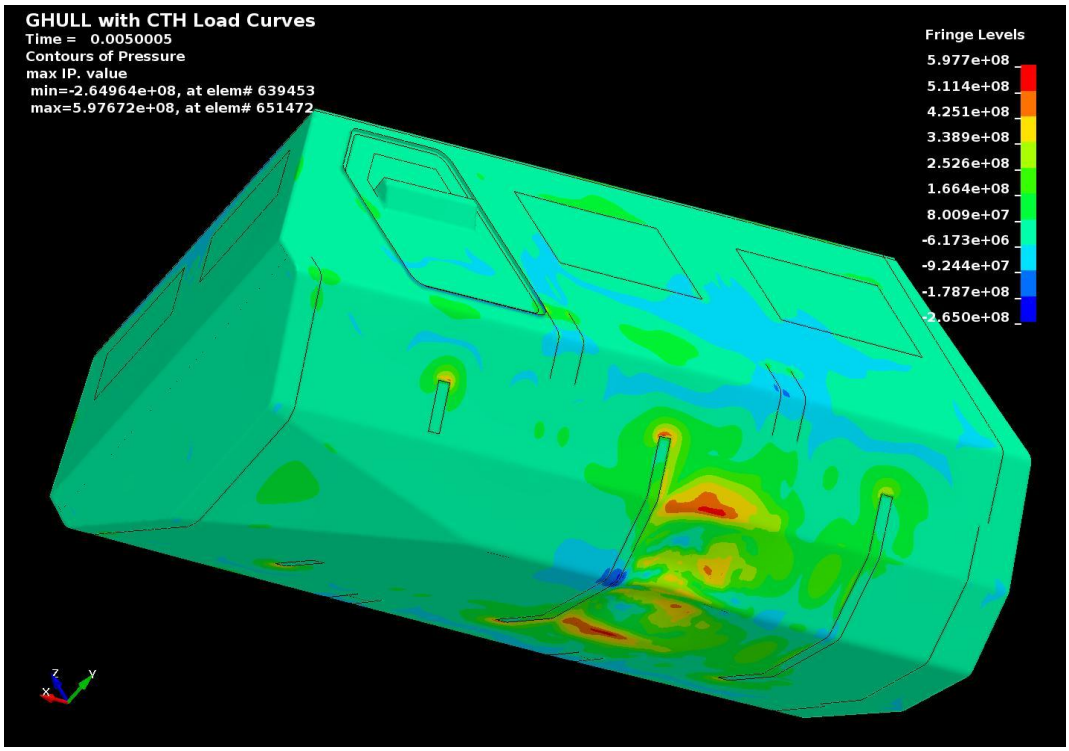

Figure 3. 25: Contours of external hull pressure at t=5e-3 seconds

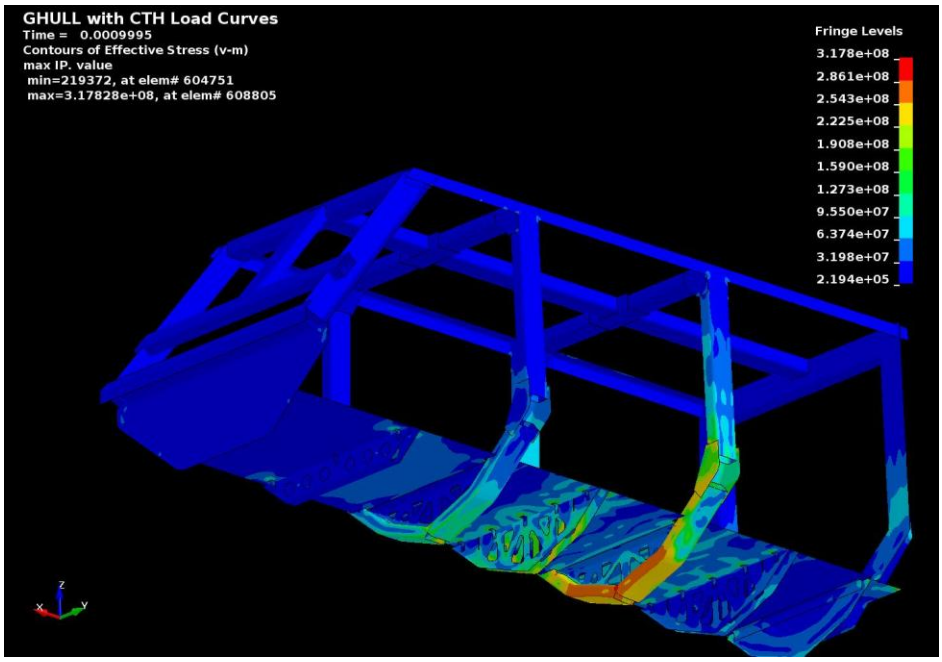

Figure 3. 26: Contours of effective stress on the internal frame at t=1e-3 seconds

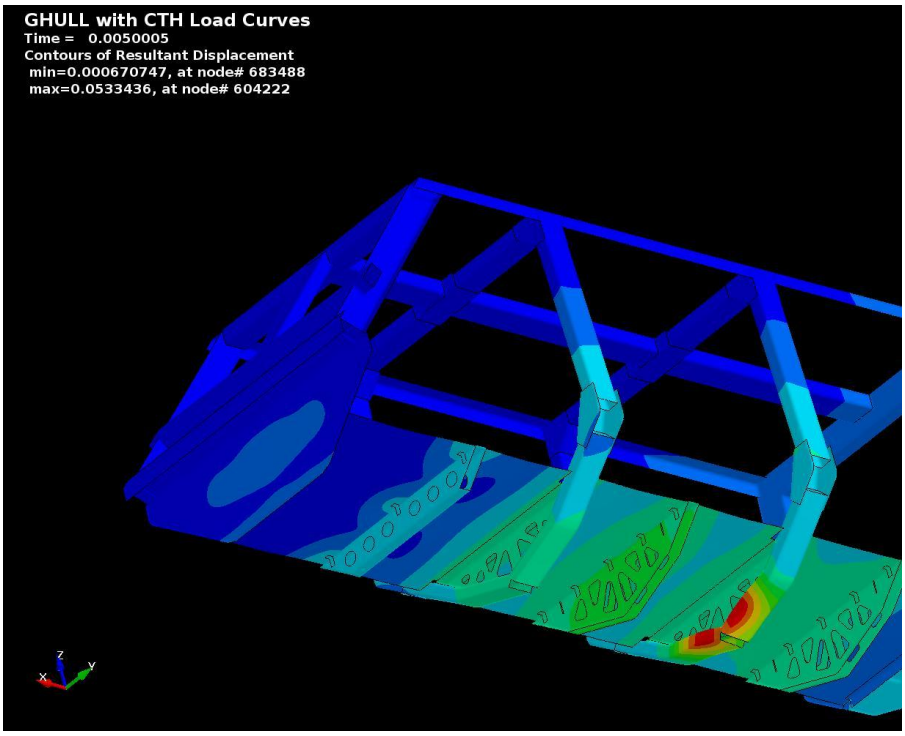

Figure 3. 27: Contours of displacement on the internal frame at t=5e-3 seconds

Section 4: Summary and Conclusions

- Under SimBRS WD0037, two enhancements to CTH (Version 9.1) were made to incorporate the ERDC HEP geo-material model and provide a one-way coupling procedure for linking CTH generated pressures to an LS-DYNA structural dynamics simulation.
- The CTH HEP model was validated for buried explosive cases using 2D witness plate simulations that compared results obtained by CTH HEP with results obtained by Kerley and Littlefield using CTH and EPIC.
- The CTH HEP model implementation was also used to simulate the ERDC IMD plate experiments. Correlations with experimental data for the three IMD soils indicated that CTH HEP provides excellent results for the wetter materials.
- Results for the IMD DRY SAND material illustrated the effect of the strength model on impulse and crater geometry and pointed to the need for a more effective strength model for the CTH HEP implementation.
- A detailed model of the IMD test configuration was also run for the WET CLAY material and compared with a fit based on the procedure developed by Kerley. The impulse from these simulations was in excellent agreement with the experiment.
- All of the tests and correlations performed to date indicate that the current implementation of the HEP model in CTH provides an accurate alternative to existing models for most soil types. However, more work needs to be done to improve the prediction of the effects of material strength for dry materials.
- The one-way coupler was implemented and verified using small witness plate simulations as well as large-scale simulations of the DRDC plate experiment and the Generic Hull experiment. The results of these simulations indicate that the one-way coupler has the potential to be an effective tool for analysis of blast effects of buried mines on vehicle underbodies.

Section 5: Recommendations

Both the HEP geo-material soil model and the one-way coupler to LS-DYNA have significant promise in the field of Underbody Blast modeling for IEDs. Evaluations should be continued to assess and improve these features, as well as incorporate them into future versions of CTH, including the production version released by Sandia National Labs. It is recommended that the the Appendices in this report be used as the starting point for the routines that need to be modified.

5.1: Technology Transition Opportunities & Drops

These enhancements to CTH v9.1 are available to any DoD agency or industry partner with the following restriction. The CTH software is owned and maintained by Sandia National Labs, NM and has been designated Export Control Information (ECI) under the International Traffic in Arms Regulations (ITAR).

5.2: Payoffs

These enhancements to CTH v9.1 are beneficial for the following reasons:

- One-way coupler with LS-DYNA:
  - CTH has a vast library of charge and soil models, and can be used to describe the blast loading into the structure, assuming a rigid interface at the underbody.
  - Once the blast loading is determined, it is applied to the Lagrangian vehicle, which runs much faster than the Arbitrary Langangian-Eulerian (ALE) formulation involving fluid-structure interaction.
  - One-way couplers have been shown to be reasonably accurate when coupled to the full two-way simulations, considering the reduced computational costs for the one-way treatment.
- Development of Hybrid-Elastic-Plastic (HEP) soil model:
  - The HEP Geo-material model from ERDC has proven to provide accurate simulations of the response of a variety of geo-materials to extreme loading due to blast, hypervelocity penetration, and ground shock.
  - Accurate material models for soils and other geo-materials are critical for analysis of shallow buried explosives such as mines and improvised explosive devices.
  - A large library of HEP models has been developed by ERDC and can be leveraged for use in CTH directly and also in the one-way coupler.

Section 6: Acknowledgements

This material is based on work supported by the U.S. Army TACOM Life Cycle Command under Contract No. W56HZV-08-C-0236, through a subcontract with Mississippi State University, and was performed for the Simulation Based Reliability and Safety (SimBRS) research program. Any opinions, finding and conclusions or recommendations in this material are those of the author(s) and do not necessarily reflect the views of the U.S. Army TACOM Life Cycle Command

The authors from MSU would like to acknowledge the support and advice provided by Dr. Ravi Thyagarajan (TARDEC/CASSI Analytics) who served as project technical monitor and advisor over the course of the project.

The authors also would like to thank Dr's Steve Akers, Ray Moral, Greg Bessette, and Kent Danielson (ERDC/GSL) and Prof. Dave Littlefield (UAB) for providing documentation on the HEP model, HEP model data for the IMD soils, EPIC correlation data, and advice on implementing the model.

Section 7: Disclaimer

Reference herein to any specific commercial company, product, process, or service by trade name, trademark, manufacturer, or otherwise does not necessarily constitute or imply its endorsement, recommendation, or favoring by the United States Government or the Dept. of the Army (DoA). The opinions of the authors expressed herein do not necessarily state or reflect those of the United States Government or the DoD, and shall not be used for advertising or product endorsement purposes.

Section 8: References/Bibliography

1. McGlaun, J., Thompson, S. and Elrick, M. "CTH: A Three-Dimensional Shock-Wave Physics Code.", International Journal of Impact Engineering, vol. 10, pp. 351-360, 1990.

2. Zimmerman, H., Wagner, M., Carney, J., Ito, Y., "Effects of Site Geology on Ground Shock Environments, Report 1, Constitutive Models for Materials I2, I3, and W1-W10," Technical Report SL-87-19, U.S. Army Engineer Waterways Experiment Station, Vicksburg, MS 1987

3. Akers, S. and Adley, M., "Constitutive Models Used to Simulate Penetration and Perforation of Concrete Targets," Proceedings of ASME Pressure Vessels and Piping Conference: Structures under Extreme Loading Conditions, PVP-vol.325, Montreal, Canada, 1996.

4. Akers, S., Ehrgott, J., Rickman, D., Williams, E., Danielson, K., "Blast Environments From Surface-Laid and Buried Bare Charges: A Joint Experimental and Simulation Effort"

5. Moral, R., Danielson, K., and Ehrgott, J., "Tactical Wheeled Vehicle Survivability: Comparison of Explosive-Soil-Air-Structure Simulations to Experiments Using the Impulse Measurement Device," Army Corp of Engineers Technical Report ERDC/GSL TR-10-27, August, 2010.

6. Danielson, K., Ehrgott, J., Moral, R., Adley, M., O'Daniel, J., Gerlach, C., Johnson, G., Littlefield, D., "Lagrangian Meshfree Methodologies for Predicting Loadings from Buried Munitions Detonations," Paper FO-002, 27th Army Science Conference, Orlando, FL, Nov. 29-Dec.2,

7. Tillotson, J., "Metallic Equations of State for Hypervelocity Impact," Technical Report GA-3216, General Atomics, San Diego, CA 1962.

8. Hertel,E. and Kerley, G., "CTH Reference Manual: The Equation of State Package," SAND98-0947, Sandia National Laboratory, Albuquerque, NM 1998

9. Hertel, E. and Kerley, G, "CTH EOS Package: Model Installation Guide," SAND98-0946, Sandia National Laboratory, Albuquerque, NM 1998

10. Brannon, R. and Wong, M.,"MIG 0.0 Model Interface Guidelines: Rules to Accelerate Installation of Numerical Models Into any Compliant Parent Code," SANDIA96-2000, Sandia National Laboratory, Albuquerque, NM 1996

11. Akers, S. A., Private Communication, December 2010.

12. Kerley, G., "Numerical Modeling of Buried Mine Explosions", ARL-CR-461, Army Research Laboratory, Aberdeen Proving Ground, MD 2001

13. Kerley, G., "The Effects of Soil Type on Numerical Simulations of Buried Mine Explosions," Report KTS02-3, Kerley Technical Services, Appomattox, VA 2002

14. Kerley, G., " On the Numerical Simulation of Buried Mine Explosions: Choosing Constitutive Models,", Report KTS05-3, Kerley Technical Services, Appomattox, VA 2005

15. Littlefield, D., "Validation of the Kerley Soil Model in CTH," presented at The 81st Shock and Vibration Symposium," Orlando FL, October 24-28, 2010

16. De Vries, D., "Thermal Properties of Soils," Chapter 7, Physics of Plant Environment, W.R Van Wijk, Ed., North-Holland Publishing Company, Amsterdam, 1966

17. Abu-Hamdeh, N., "Thermal Properties of Soils as Affected by Density and Water Content," Biosystems Engineering, Vol. 86, No. 1, pp. 97-192, 2003

18. Hendrickx, J., van Dam, R., Borchers, B., Curtis, J., Lensen, H., Harmon, R., "Worldwide distribution of soil dialectric and thermal properties," Proceeding SPIE 5089, 1158(2003), Detection and Remediation Technologies for Mine and Mine-like Targets, VIII.

19. Scott, H., Soil Physics, Agricultural and Environmental Applications, Iowa State University Press, Ames, IA, 2002

20. Ehrgott, J., "Tactical Wheeled Vehicle Survivability: Results of Experiments to Quantify Aboveground Impulse," Army Corp of Engineers Technical Report ERDC/GSL TR-10-7, March 2010.

21. Erhgott, J, et al., "Tactical Wheeled Vehicle Survivability: Construction and Characterization of Dry Sand Testbeds in Bare Charge Experiments," Army Corp of Engineers Technical Report ERDC/GSL TR-10-15, March 2010.

22. Erhgott, J, et al., "Tactical Wheeled Vehicle Survivability: Construction and Characterization of Intermediate-Air-Voids, Silty Sand Testbeds in Bare Charge Experiments," Army Corp of Engineers Technical Report ERDC/GSL TR-10-16, April 2010.

23. Erhgott, J, et al., "Tactical Wheeled Vehicle Survivability: Construction and Characterization of Wet Clay Testbeds in Bare Charge Experiments," Army Corp of Engineers Technical Report ERDC/GSL TR-10-17, April 2010.

24. Williams, K., McClennan, S., Durocher, R, St-Jean, B., Trembelay, J., "Validation of a Loading Model for Simulating Blast Mine Effects on Armoured Vehicles," 7th International LS-DYNA Users Conference, Detroit, MI 2002.

25. Bessette, Greg, Private Communication, November, 2011.

26. Silling, S.A., "CTH Reference Manual: Johnson-Holmquist Ceramic Model," Report SAND92-0576, June, 1996.

27. Littlefield, D.L, Harvey, J.P, and Kulatha, S., “Implementation of a Uni-directional Coupling Interface into CTH,” HPCMP PET Project Report, 2006.

28. Crawford, D.A., “CHSSI CTH Presto One-Way Coupling Procedure,” CTH Technical Note, January, 2007.

29. Thompson, D., Luke, E., Moore, C., Remotique, M., Tong, X.L., Weed, R., and Ivancic, P., “Enhance Simulation of Blast-Vehicle Interactions using Loci/BLAST and LS-DYNA,”, Final Report, SimBRS EWD No:, WD0034, June, 2012.

30. Dooge, Dooge D, Dwarampudi R, Schaffner G, Miller A, Thyagarajan R, Vunnam M, Babu V, 2011, “Evolution of Occupant Survivability Simulation Framework Using FEM-SPH Coupling,” 2011 NDIA Ground Vehicle System Engineering and Technology Symposium (GVSETS), MSTV Mini-Symposium Paper, August 9-11, Dearborn, Michigan

31. Toussaint, Genevieve and Bouamoul, Amal, “Comparison of ALE and SPH Methods for Simulating Mine Blast Effects on Structures,” Technical Report, DRDC Valcartier TR 2010-0326, December, 2010.

32. Bessette, G. Vaughan, C., Bell, R., Yarrington, P., and Attaway, S., “Zapotec: A Coupled Eulerian-Lagrangian Computer Code, Methodology and Users Manual, Version 1.0,” Sandia Technical Report, Sandia National Laboratories, 2003.

33. Schaffner, G and Miller, A, “Mitigation of Occupant Acceleration in a Mine-Resistant Ambush-Protected Vehicle Blast Event using an Optimized Dual-Hull Approach,” 2012 NDIA Ground Vehicle System Engineering and Technology Symposium (GVSETS), MSTV Mini-Symposium Paper, August 14-16, Dearborn, Michigan.

Section 9: Appendices

APPENDIX A: Description of HEP Model Software and CTH Code Modifications

A.1 Overview

As previously stated in this report, the CTH HEP EOS implementation followed the CTH EOS implementation guidelines outlined by Hertel and Kerley [9]. The procedure for implementing a new EOS in CTH can be summarized in the following steps:

1. Define a material number for the new material. The CTH HEP EOS was defined to be model number 27 in CTH 9.1

2. Modify CTH routine EOSUIP to assign the number and read the input data specific to the selected model number.

3. Create a new routine to check and verify the input data and modify the CTH routine EOS1SI to call the data check routine based on the selected model number

4. Create a new routine to assign "extra variables" needed by the HEP and modify CTH routine EOS1SK to call the new extra variable routine based on the selected model number

5. Create two new driver routines for the underlying EOS routines. The first of these driver routines is as a scalar version of the EOS. It takes in density and temperature and returns pressure, internal energy, and sound speed. The scalar routine is called once for each cell containing an HEP material. The second driver routine is a vectorized EOS routine that takes in density and energy and returns pressure, temperature and sound speed. The vectorized version of the EOS driver takes in data from an entire array of cells and processes the data in a vector loop.

6. Modify CTH routine EOS to call the scalar version of the EOS driver and routine EOSMRE to call the vector version of the EOS driver

7. Add a default input block for the new EOS to the CTH EOS data file. The format for the input block requires a list of keywords that will identify the input

A similar procedure for implementing a constitutive (strength) model in CTH is not as well documented. As with the EOS, the first task is to pick a material number. Unlike the EOS, most of the modifications to existing CTH routines are implemented in the form of several include files in C header file format. These include file perform a variety of tasks such as setting dimensions of arrays used by the input processor, defining extra variables and initial values, and calling the main driver routine for the elastic-plastic strength model of a particular material. The majority of the include files are used in the

UINCHK and UINEP routines that handle data checking and data input. The main elastic-plastic driver routine for a material is called from ELSG. The definition of extra variables is performed in UINISV.

The following section lists both the new routines that make up the HEP EOS and strength model and gives a short description of what they do or the modification made to an existing CTH routine. The directory containing the source code for the new or modified routine is given in parenthesis after the source file name

A.2 New EOS routines

The following routine are new routines specific to the HEP EOS implementation. Most of the new software described in the following sections was written in Fortran 2003 free field format signaled by the F90 file extension. A new CTH subdirectory (/src/raw) was created to hold the new HEP model software along with the "one-way" coupler software

A.2.1 hep_constants_module.F90 (/src/modules)

Fortran 2003 module containing global data used by the HEP model and support routines.

A.2.2 eshepe.F90 (/src/raw)

The "vectorized" EOS driver that takes in density and energy and returns pressure, temperature, and sound speed. Called by EOSMRE.

A.2.3 eshept.F90 (/src/raw)

The "scalar" EOS driver that takes in density and temperature and returns pressure, energy, and sound speed. Called by EOS

A.2.4 eshepi.F90 (/src/raw)

The data check routine for the HEP EOS model. Called by EOS1SI.

A.2.5 eshepx.F90 (/src/raw)

The HEP EOS extra variable routine. Called by EOS1SK

A.2.6 hepeos.F90 (/src/raw)

The main HEP EOS routine. Calls HEPHydroStat to compute energy independent component of pressure. Called by eshepe.F90 and eshepe.F90

A.2.7 HEPHydroStat.F90

Computes the energy independent component of the HEP pressure. Called by hepeos.F90

A.3 CTH routines modified for HEP EOS model

A.3.1 eosuip.F (/src/eos)

Added CTH HEP model as model number 27.

A.3.2 eos1si.F (/src/eos)

Added call to eshepi.F90 check routine

A.3.3 eos1sk.F (/src/eos)

Added call to eshepx.F90 extra variable routine

A.3.4 eos.F (/src/eos)

Added call to eshept.F scalar EOS driver

A.3.5 eosmre.F (/src/eos)

Added call to eshepe.F vector EOS driver

A.4 New HEP Elastic-Plastic Model Routines

A.4.1 hepchk.F90 (/src/raw)

Data check routine for HEP EP model. Called in uinchk.F

A.4.2 hepepx.F90 (/src/raw)

Extra variable routine for HEP EP model. Called by uinisv.F

A.4.3 hepepdr.F90 (/src/raw)

Driver routine for HEP EP routines. Calls SHEPYieldFunction and SHEPShearModulus. Called by elsg.F

A.4.4 SHEPYieldFunction.F90 (/src/raw)

Computes SHEP yield strength. Called by hepepdr.F90

A.4.5 SHEPShearModulus.F90 (/src/raw)

Computes SHEP shear modulus. Called by hepepdr.F90

A.5 CTH routines modified for HEP EP model

A.5.1 uinchk.F (/src/reb)

Added m27p1.h include file

A.5.2 uinep.F (/src/reb)

Added m27p0a.h, m27p0b.h, m27p0c.h, and m27p0d.h include files.

A.5.3 uinisv.F (/src/sas)

Added m27p2.h include file.

A.5.4 elsg.F (/src/sas)

Added m27p3.h include file

A.5.5 elygp.F (/src/sas)

Added modifications to reference SHEP yield and shear modulus values.

A.6 New HEP EP model include files in /include/cth

A.6.1 m27p0a.h

Sets material model number, material name, title and MIG routine array dimensions.

A.6.2 m27p0b.h

Contains call to MIG RDATA routine

A.6.3 m27p0c.h

Contains call to MIG LOOKFK routine

A.6.4 m27p0d.h

Initializes default EP routine values such as TMELT and YLDVM

A.6.5 m27p1.h

Contains call to hepchk.F data check routine

A.6.6 m27p2.h

Contains call to hepepx.F extra variable routine.

A.6.7 m27p3.h

Contains call to hepepdr.F HEP EP model driver routine

APPENDIX B: Description of CTH-LS-DYNA coupler software and CTH code modifications

B.1 Overview

The CTH-LS-DYNA coupler was initially based on the software developed by Littlefield et al. [27]. Over the course of the development of the current coupler much of this software was either highly modified or completely rewritten. However, there are a few routines that are have minor modifications or are unchanged form the original code. Most of the new code for the coupler deals with processing LS-DYNA LOAD_SEGMENT and LOAD_SHELL keyword inputs in CTH, extracting time averaged pressures for a CTH rigid material and saving them to a history file named femh. Other routines handle reading and writing restart files and post-processing the data in the femh file to generate a file containing LS-DYNA DEFINE_CURVE input. Although the new code is focused solely on LS-DYNA support, the original code also supported DYNA3D. Some of the logic for DYNA3D support was maintained but has never been tested.

A typical CTH run using the coupler software performs the following tasks

1. The fem/endfem block in the users main CTH input file is read by UINFEM and various flags and values are set based on the users input.

2. The femh file is created if it doesn't already exist.

3. The users LS-DYNA input defining LOAD_SEGMENT or LOAD_SHELL inputs is read and used to define CTH cell locations closest to the target CTH LOAD_SEGMENT or LOAD_SHELL

4. As CTH runs to the prescribed stop time, the coupler software computes a time average pressure to be applied to the target LS-DYNA LOAD_SEGMENT and LOAD _SHELL element faces. The algorithm and some of the code that performs this task was borrowed from the existing CTH rigid material model and modified for use by the coupler.

5. The computed pressures are saved in the femh file at a user defined frequency.

6. At the end of the job, the femh file is scanned in a post-processing step and the file containing the LS-DYNA DEFINE_CURVE input is generated.

Steps 3 and 4 are performed in parallel for mpicth runs. All other steps are done by the parent process. The current version of the software is limited to LOAD_SEGMENT and LOAD_SHELL inputs. This can lead to extremely large DEFINE_CURVE files. An alternate approach that would allow the use of LOAD_SEGMENT_SETS to reduce the number of generated load curves is being investigated but is not in the current release of the software. The following sections describe the new software and the CTH routines that were modified to support the coupler. The directory containing the new software is shown in parentheses.

B.2 New CTH-LS-DYNA coupler software

B.2.1 femesr.F/femsew.F (/src/raw)

Routines to read and write coupler restart data. Called by dbmwtf.F

B.2.2 femop.F (/src/raw)

Executive routine for opening coupler input and output files

B.2.3 femini.F (/src/raw)

Initialization routine

B.2.4 fempst.F (/src/raw)

Performs post processing of femh file data and generation of DEFINE_CURVE data

B.2.5 femsur.F90 (/src/raw)

Computes surface normals and areas of target LS-DYNA LOAD_SEGMENT and LOAD_SELL surfaces

B.2.6 femwrt.F90 (/src/raw)

Writes data to the femh file at a user defined frequency

B.2.7 setfem.F90 (/src/raw)

Selects type of coupling. Original version of coupler had support for DYNA3D. Kept for possible future extension of the code to reinstate DYNA3D support

B.2.8 seting.F (/src/raw)

Read in data from DYNA3D files to define load curves. Kept for possible future extension to reinstate DYNA3D support

B.2.9 setlsd.F (/src/raw)

Reads the LS-DYNA input keyword file. Parses files for LOAD_SEGMENT, LOAD_SHELL and NODE keywords. Computes array dimensions and allocate memory for coupler arrays.

B.2.10 settra.F (/src/raw)

Finds location of CTH cell centers nearest to the target LS-DYNA surface

B.2.11 hfeme.F (/src/raw)

Database manager for hfemeds routine

B.2.12 hfemeds.F (/src/raw)

Extracts pressures for rigid target material and computes time averaged pressure

B.2.13 uinfem.F (/src/raw)

Reads fem/endfem block input and sets flags needed by coupler

B.2.14 countLoadSegs.F90, countLoadShells.F90, countNodes.F90 (/src/raw)

Routines that count the number of LOAD_SEGMENT, LOAD_SHELL, and NODE inputs. These numbers are used for allocating memory for coupler arrays.

B.2.15 parseLoadSegs.F90, parseLoadShells.F90, parseNodes.F90 (/src/raw)

Reads LS-DYNA LOAD_SEGMENT, LOAD_SHELL, and NODE inputs

B.2.16 checkFemSym.F90 (/src/raw)

Checks to see if I and J direction symmetry flags where set in fem/endfem block and adjust node x and y values defined in the LOAD_SEGMENT, NODE, and LOAD_SHELL input.

B.2.17 findNodeIndex.F90 (/src/raw)

Provides a map between node and element indices

B.2.18 getShellIndex.F90 (/src/raw)

Gets index for shell elements

B.3 CTH routines modified for the CTH-LS-DYNA coupler

B.3.1 dbmwtf.F (/src/dbm)

Calls femesr and femesw restart data I/O routines

B.3.2 celop.F (/src/jmm)

Calls fempst at the end of a CTH run. Also, main CTH subroutine that controls the global solution process.

B.3.3 edende.F (/src/jmm)

Calls femwrt at the end of each step to write data to femh

B.3.4 uins.F (/src/jmm)

Calls uinfem to read fem/endfem input block data. Also calls setfem to define type of coupling.

B.3.5 erdrv.F (/src/rlb)

Calls femfop, hfeme and femweb

B.3.6 gcntrl.F (/src/slt)

Calls uinfem and setfem. Part of the old mpigen software

Section 10: Distribution List

- Mr. Sudhakar Arepally, Associate Director, Analytics, US Army TARDEC
- Mr. Craig Barker, Team Leader, SLAD, US Army Research Labs
- Mr. Chuck Coutteau, Deputy Executive Director, Ground Systems Engineering Assessment and Assurance/Systems Integration and Engineering, US Army TARDEC
- Dr. David Crawford, CTH Technical Lead, Computational Thermal and Fluid Sciences Department, Sandia National Labs, DoE
- Dr. Kent Danielson, Engineering Systems & Materials Division Research Group, Geotechnical and Structures Lab, Engineer Research and Development Center (ERDC), Army Core of Engineers
- Mr. Paul Decker, Deputy Chief Scientist, US Army TARDEC
- Mr. Ed Fioravante, Team Leader, WMRD, US Army Research Labs
- Dr. David Gorsich, Chief Scientist, US Army TARDEC
- Mr. Pat Horton, Program Manager, UBM/T&E, SLAD, US Army Research Labs
- Dr. Steve Knott, Associate Director, TARDEC/GSS, US Army TARDEC
- Dr. Scott Kukuck, PM/Blast Institute, WMRD, US Army Research Labs
- Dr. David Lamb, STE/Analytics, US Army TARDEC
- Mr. Madan Vunnam, Team Leader, Analytics/EECS, US Army TARDEC
- TARDEC TIC (Technical Information Center) archives, US Army TARDEC